



US Army Corps  
of Engineers

TECHNICAL REPORT CERC-87-15

# ANALYTICAL SOLUTIONS OF THE ONE-LINE MODEL OF SHORELINE CHANGE

by

Magnus Larson, Hans Hanson

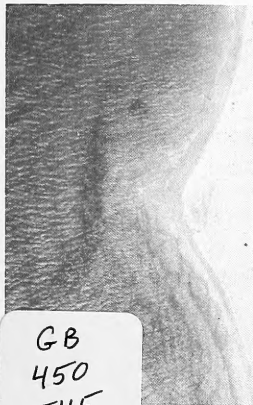
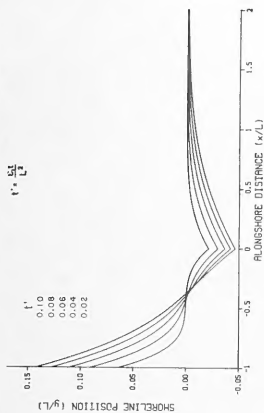
Department of Water Resources Engineering  
Institute of Science and Technology  
University of Lund  
Box 118, Lund, Sweden S-221-00

and

Nicholas C. Kraus

Coastal Engineering Research Center

DEPARTMENT OF THE ARMY  
Waterways Experiment Station, Corps of Engineers  
PO Box 631, Vicksburg, Mississippi 39180-0631



**DATA LIBRARY**  
Woods Hole Oceanographic Institution



October 1987

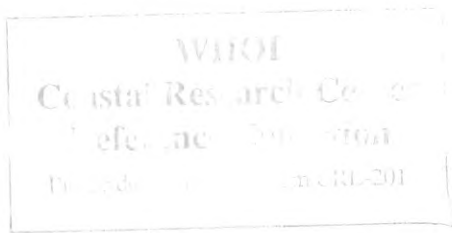
Final Report

Approved For Public Release, Distribution Unlimited

GB  
450  
T45  
no.  
CERC-87-15



Prepared for DEPARTMENT OF THE ARMY  
US Army Corps of Engineers  
Washington, DC 20314-1000  
Under Coastal Sediment Transport Processes  
Work Unit 324-1



Destroy this report when no longer needed. Do not return  
it to the originator.

The findings in this report are not to be construed as an official  
Department of the Army position unless so designated  
by other authorized documents.

The contents of this report are not to be used for  
advertising, publication, or promotional purposes.  
Citation of trade names does not constitute an  
official endorsement or approval of the use of  
such commercial products.

Unclassified  
SECURITY CLASSIFICATION OF THIS PAGE

| REPORT DOCUMENTATION PAGE   |  |  |  |          | Form Approved<br>OMB No 0704-0188<br>Exp. Date: Jun 30, 1986 |
|---|--|--|--|----------|--|
| 1a. REPORT SECURITY CLASSIFICATION<br>Unclassified  |  | 1b. RESTRICTIVE MARKINGS   |  |          |  |
| 2a. SECURITY CLASSIFICATION AUTHORITY   |  | 3. DISTRIBUTION / AVAILABILITY OF REPORT<br>Approved for public release; distribution unlimited. |  |          |  |
| 2b. DECLASSIFICATION / DOWNGRADING SCHEDULE   |  | 5. MONITORING ORGANIZATION REPORT NUMBER(S)  |  |          |  |
| 4. PERFORMING ORGANIZATION REPORT NUMBER(S)<br>Technical Report CERC-87-15  |  | 7a. NAME OF MONITORING ORGANIZATION  |  |          |  |
| 6a. NAME OF PERFORMING ORGANIZATION<br>USAEWES, Coastal Engineering Research Center   | 6b. OFFICE SYMBOL<br>(if applicable)       | 7b. ADDRESS (City, State, and ZIP Code)  |  |          |  |
| 6c. ADDRESS (City, State, and ZIP Code)<br>PO Box 631<br>Vicksburg, MS 39180-0631   |  | 9. PROCUREMENT INSTRUMENT IDENTIFICATION NUMBER  |  |          |  |
| 8a. NAME OF FUNDING / SPONSORING ORGANIZATION<br>US Army Corps of Engineers   | 8b. OFFICE SYMBOL<br>(if applicable)       | 10. SOURCE OF FUNDING NUMBERS  |  |          |  |
| 8c. ADDRESS (City, State, and ZIP Code)<br>Washington, DC 20314-1000  |  | PROGRAM ELEMENT NO.  | PROJECT NO.  | TASK NO. | WORK UNIT ACCESSION NO<br>324-1                              |
| 11. TITLE (Include Security Classification)<br>Analytical Solutions of the One-Line Model of Shoreline Change   |  |  |  |          |  |
| 12. PERSONAL AUTHOR(S)<br>Larson, Magnus; Hanson, Hans; Kraus, Nicholas C.  |  |  |  |          |  |
| 13a. TYPE OF REPORT<br>Final report   | 13b. TIME COVERED<br>FROM Jul 86 TO Dec 86 | 14. DATE OF REPORT (Year, Month, Day)<br>October 1987  | 15. PAGE COUNT<br>100  |          |  |
| 16. SUPPLEMENTARY NOTATION<br>Available from National Technical Information Service, 5285 Port Royal Road, Springfield, VA 22161.   |  |  |  |          |  |
| 17. COSATI CODES  |  | 18. SUBJECT TERMS (Continue on reverse if necessary and identify by block number)                |  |          |  |
| FIELD   | GROUP                                      | SUB-GROUP  |  |          |  |
|   |  |  | Coast changes (LC) Mathematical models (LC)<br>Beach erosion (LC) Shore-lines (LC) |          |  |
| 19. ABSTRACT (Continue on reverse if necessary and identify by block number)  |  |  |  |          |  |
| <p>This report presents more than 25 closed-form solutions of the shoreline change mathematical model for simulating the evolution of sandy beaches. The governing equation is developed in a general form, and the assumptions and techniques used to arrive at tractable closed-form solutions are described. Previous solutions are reviewed, and many new solutions are derived. Solutions for beach evolution with and without the influence of coastal structures are given that cover situations involving beach fill of almost arbitrary initial shapes, sand mining, river discharges, groins and jetties, detached breakwaters, and seawalls. Techniques for combining and extending the solutions are discussed. Appendixes provide details of mathematical techniques used and complete derivations of selected new solutions. Such analytical solutions can provide a simple and economical means to make a quick qualitative evaluation of shoreline response under a wide range of environmental and engineering conditions.</p> |  |  |  |          |  |
| 20. DISTRIBUTION / AVAILABILITY OF ABSTRACT<br><input checked="" type="checkbox"/> UNCLASSIFIED/UNLIMITED <input type="checkbox"/> SAME AS RPT. <input type="checkbox"/> DTIC USERS   |  | 21. ABSTRACT SECURITY CLASSIFICATION<br>Unclassified   |  |          |  |
| 22a. NAME OF RESPONSIBLE INDIVIDUAL   |  | 22b. TELEPHONE (Include Area Code)   | 22c. OFFICE SYMBOL   |          |  |

DD FORM 1473, 84 MAR

83 APR edition may be used until exhausted.  
All other editions are obsolete.

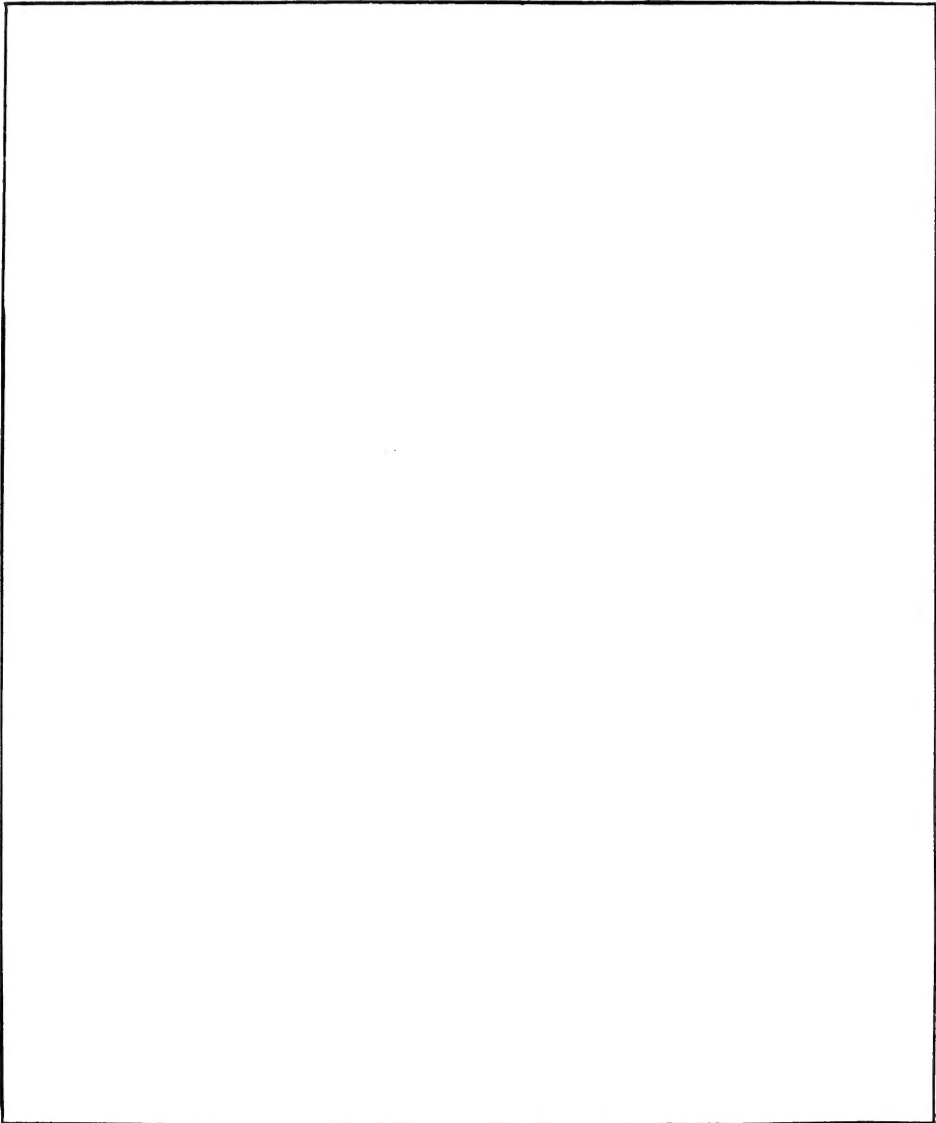
SECURITY CLASSIFICATION OF THIS PAGE

Unclassified

MBL/WHOI Library  
 003011000802

Unclassified

**SECURITY CLASSIFICATION OF THIS PAGE**



Unclassified

**SECURITY CLASSIFICATION OF THIS PAGE**

## PREFACE

The investigation described in this report was authorized as a part of the Civil Works Research and Development Program by the Office, Chief of Engineers (OCE), US Army Corps of Engineers. The work was performed under the Coastal Sediment Transport Processes Work Unit 324-1, Shore Protection and Restoration Program, at the Coastal Engineering Research Center (CERC) of the US Army Engineer Waterways Experiment Station (WES). Messrs. John H. Lockhart, Jr., and John G. Housley were the OCE Technical Monitors.

The study was conducted from 1 July 1986 through 31 December 1986 by Dr. Nicholas C. Kraus, Research Physical Scientist and Principal Investigator, Coastal Sediment Transport Processes Work Unit, Research Division (CR), CERC, in conjunction with related engineering studies by Messrs. Magnus Larson and Hans Hanson of the University of Lund, Sweden. This report presents the overall results of these efforts. The CERC portion of the study was conducted under general supervision of Dr. James R. Houston, Chief, CERC; Mr. Charles C. Calhoun, Jr., Assistant Chief, CERC; and Dr. Charles L. Vincent, Program Manager, Shore Protection and Restoration Program, CERC; and under direct supervision of Mr. H. Lee Butler, Chief, CR, CERC. Work at the University of Lund was performed under general supervision of Dr. Gunnar Lindh, Head, Department of Water Resources Engineering, Institute of Science and Technology. Mr. Bruce A. Ebersole provided technical review. This report was edited by Ms. Shirley A. J. Hanshaw, Information Technology Laboratory, Information Products Division, WES.

COL Dwayne G. Lee, CE, was Commander and Director of WES during publication of this report. Dr. Robert W. Whalin was Technical Director.

## CONTENTS

|   | <u>Page</u> |
|---|-------------|
| PREFACE.....  | 1           |
| LIST OF FIGURES.....  | 3           |
| PART I: INTRODUCTION.....   | 6           |
| Background.....   | 6           |
| One-Line Theory.....  | 7           |
| Overview of Previous Analytical Work.....   | 12          |
| General Approach in the Present Work.....   | 16          |
| PART II: SOLUTIONS FOR SHORELINE EVOLUTION WITHOUT<br>COASTAL STRUCTURES.....   | 18          |
| General Formal Solution.....  | 18          |
| Finite Rectangular Beach Fill.....  | 19          |
| Semi-Infinite Rectangular Beach Fill.....   | 23          |
| Rectangular Cut in a Beach.....   | 24          |
| Triangular-Shaped Beach.....  | 26          |
| Trapezoidal-Shaped Beach.....   | 27          |
| Semicircular-Shaped Beach.....  | 30          |
| Semicircular Cut in a Beach.....  | 34          |
| Rhythmic Beach.....   | 36          |
| Sand Discharge from a River Acting as a Point Source.....   | 37          |
| Sand Discharge from a River Mouth of Finite Length.....   | 41          |
| PART III: SOLUTIONS FOR SHORELINE EVOLUTION INVOLVING<br>COASTAL STRUCTURES.....  | 46          |
| Shoreline Change at Groins and Jetties.....   | 46          |
| Initially Filled Groin System.....  | 53          |
| Shoreline Change at a Detached Breakwater.....  | 55          |
| Shoreline Change at a Seawall.....  | 60          |
| Shoreline Change at a Jetty, Including Diffraction.....   | 63          |
| REFERENCES.....   | 71          |
| APPENDIX A: A SHORT INTRODUCTION TO THE LAPLACE<br>TRANSFORM TECHNIQUE.....   | A1          |
| APPENDIX B: SHORELINE EVOLUTION DOWNDRIFT OF A GROIN WITH<br>BYPASSING REPRESENTED BY AN EXPONENTIAL FUNCTION.....                    | B1          |
| APPENDIX C: SHORELINE EVOLUTION BEHIND A DETACHED BREAKWATER.....   | C1          |
| APPENDIX D: SHORELINE EVOLUTION IN THE VICINITY OF A SEAWALL<br>WHERE FLANKING OCCURS.....  | D1          |
| APPENDIX E: SHORELINE EVOLUTION DOWNDRIFT OF A JETTY IF AN<br>ARBITRARY NUMBER OF SOLUTION AREAS IS USED TO<br>MODEL DIFFRACTION..... | E1          |
| APPENDIX F: SHORELINE EVOLUTION BEHIND A JETTY FOR LINEARLY<br>VARYING BREAKING WAVE ANGLE.....                                       | F1          |
| APPENDIX G: SHORELINE EVOLUTION BEHIND A JETTY FOR EXPONENTIALLY<br>VARYING BREAKING WAVE ANGLE.....                                  | G1          |
| APPENDIX H: NOTATION.....   | H1          |

LIST OF FIGURES

| <u>No.</u> |  | <u>Page</u> |
|------------|--|-------------|
| 1          | Schematic illustration of a hypothetical equilibrium beach profile.....  | 8           |
| 2          | Definition sketch for geometric properties at a specific location as related to shoreline change.....  | 10          |
| 3          | Comparison between experimental and theoretical shoreline evolution.....   | 13          |
| 4          | Definition sketch for the two-line theory.....   | 14          |
| 5          | Two-line theory solution for a groin system.....   | 15          |
| 6          | Shoreline evolution between two groins initially filled with sand.....   | 16          |
| 7          | Shoreline evolution of an initially rectangular beach fill exposed to waves arriving normal to shore.....  | 19          |
| 8          | Percentage of sand volume lost from a rectangular fill as a function of dimensionless time.....  | 22          |
| 9          | Shoreline evolution when sand is supplied at $x = 0$ to maintain a specific beach width $y_0$ .....  | 23          |
| 10         | Shoreline evolution of an initially semi-infinite rectangular beach.....   | 24          |
| 11         | Shoreline evolution of a rectangular cut in an infinite beach of width $y_0$ .....   | 25          |
| 12         | Shoreline evolution of an initially triangular beach.....  | 27          |
| 13         | Comparison between analytical solution with the linearized transport equation and numerical solution with the original transport equation for a triangular beach fill (for height-to-width ratios of 1.0 and 0.5)..... | 28          |
| 14         | Shoreline evolution of an initially trapezoidal beach form.....  | 29          |
| 15         | Shoreline of arbitrary shape approximated by $N$ straight lines.....   | 30          |
| 16         | Semicircular-shaped beach approximated by a polygon.....   | 31          |
| 17         | Shoreline evolution of an initially semicircular beach.....  | 32          |
| 18         | Definition sketch for a circular segment-shaped beach.....   | 33          |

| <u>No.</u> |   | <u>Page</u> |
|------------|---|-------------|
| 19         | Shoreline evolution of an initially circular segment-shaped beach ( $\alpha = 45$ deg).....   | 34          |
| 20         | Comparison between analytical and numerical solutions for the case of a circular segment-shaped beach.....  | 35          |
| 21         | Shoreline evolution of an initially semicircular cut in a beach.....  | 35          |
| 22         | Shoreline evolution of an initially circular segment cut in a beach ( $\alpha = 45$ deg).....   | 36          |
| 23         | Shoreline evolution of an initially cosine-shaped beach (a distance of one beach cusp height added to the shoreline position).....  | 37          |
| 24         | Shoreline evolution in the vicinity of a river discharging sand and acting as a point source.....   | 39          |
| 25         | Shoreline evolution in the vicinity of a river discharging sand with a periodic variation in strength as a function of time ( $\omega L^2/\epsilon = 2$ , $\phi = 0$ , $q_s/Q_o = q_o/Q_o = 0.5$ )..... | 40          |
| 26         | Shoreline evolution in the vicinity of a sand-discharging river mouth of finite width.....  | 43          |
| 27         | Maximum delta growth from a sand-discharging river mouth of finite length.....  | 44          |
| 28         | Definition sketch for the case of a groin.....  | 47          |
| 29         | Shoreline evolution updrift of a groin which is totally blocking the transport of sand alongshore.....  | 48          |
| 30         | Shoreline evolution downdrift of a groin with bypassing described by $Q_B(1 - e^{-\gamma t})$ ( $Q_B/Q_o = 0.7$ , $\alpha_o = 0.4$ rad , $\gamma L^2/\epsilon = 2$ ).....                               | 51          |
| 31         | Comparison between analytical and numerical solutions of shoreline evolution updrift of a groin with incident breaking wave angle 20 deg.....   | 52          |
| 32         | Comparison between analytical and numerical solutions of shoreline evolution updrift of a groin with incident breaking wave angle 45 deg.....   | 52          |
| 33         | Shoreline evolution between two groins initially filled with sand ( $L/W = 0.33$ , $\alpha_o = 0.25$ rad).....  | 54          |



| <u>No.</u> |  | <u>Page</u> |
|------------|--|-------------|
| 34         | Bypassing sand transport rate at the downdrift end of a groin<br>x = W as a function of time.....  | 55          |
| 35         | Definition sketch for the problem of shoreline change in the<br>vicinity of a detached breakwater.....   | 56          |
| 36         | Initial shoreline evolution in the vicinity of a shore-parallel<br>detached breakwater ( $\delta = 0.5$ , $\alpha_{o1} = 0.4$ rad , $\alpha_{o2} = 0$ ).....                                     | 59          |
| 37         | Final shoreline position in the vicinity of a shore-parallel<br>detached breakwater ( $\delta = 0.5$ , $\alpha_{o1} = 0.4$ rad , $\alpha_{o2} = 0$ ).....  | 60          |
| 38         | Definition sketch for a semi-infinite seawall for which no<br>erosion occurs behind the seawall.....   | 61          |
| 39         | Definition sketch for a semi-infinite seawall for which erosion<br>occurs behind the seawall.....  | 61          |
| 40         | Shoreline evolution in the vicinity of a seawall where<br>erosion and flanking may occur behind it ( $\alpha_{o1} = 0.2$ rad ,<br>$\alpha_{o2} = 0.4$ rad , $\delta = 0.6$ ).....                | 63          |
| 41         | Definition sketch for shoreline evolution downdrift of a jetty<br>for which a finite number of solution areas is used to<br>model diffraction.....   | 66          |
| 42         | Shoreline evolution in the vicinity of a groin for variable sand<br>transport rate conditions (two solution areas; $\delta = 0.5$ ,<br>$\alpha_{o1} = -0.1$ rad , $\alpha_{o2} = -0.4$ rad)..... | 67          |
| 43         | Shoreline evolution behind a jetty with linear variation in<br>breaking wave angle in the shadow zone ( $\alpha_v = -0.1$ rad ,<br>$\alpha_H = 0.4$ rad).....                                    | 69          |
| 44         | Shoreline evolution behind a jetty with exponential variation in<br>breaking wave angle ( $\alpha_m = 0.4$ rad , $\gamma L = 1$ ).....   | 70          |

ANALYTICAL SOLUTIONS OF THE ONE-LINE MODEL  
OF SHORELINE CHANGE

PART I: INTRODUCTION

Background

1. Mathematical modeling of shoreline change has proven to be a useful engineering technique for understanding and predicting the evolution of the plan shape of sandy beaches. In particular, mathematical models provide a concise, quantitative means of describing systematic trends in shoreline evolution commonly observed at groins, jetties, and detached breakwaters and produced by coastal engineering activities such as beach nourishment and sand mining.

2. Qualitative and quantitative understanding of idealized shoreline response to the governing processes is necessary in investigations of beach behavior. By developing analytical or closed-form solutions originating from mathematical models which describe the basic physics involved to a satisfactory level of accuracy, essential features of beach response may be derived, isolated, and more readily comprehended than in complex approaches such as numerical and physical modeling. Also, with an analytical solution as a starting point, it is possible to estimate, rapidly and economically, characteristic quantities associated with the phenomenon, such as the time elapsed before bypassing of a groin occurs, percentage of volume lost from a beach fill, and growth of a salient (emerging tombolo) behind a detached breakwater. Another useful property is the capability to obtain equilibrium conditions from asymptotic solutions. Closed-form solutions for shoreline change can also be used as a teaching aid. However, the complexity of beach change implies that results obtained from a model should be interpreted with care and with awareness of the underlying assumptions. Closed-form mathematical models cannot be expected to provide quantitatively accurate solutions to problems involving complex boundary conditions and wave inputs. In engineering design, a numerical model of shoreline evolution would be more appropriate.

3. The equations describing shoreline evolution fast become excessively complicated to permit analytical treatment if too many phenomena are described

in one formulation. Therefore, to obtain a closed-form solution to shoreline change, a simple mathematical formulation has to be used, but one which still preserves the important mechanisms involved. The one-line (denoting the shoreline) theory was introduced by Pelnard-Considère (1956), and it has been demonstrated to be adequate in this respect. Considerable numerical modeling of long-term shoreline evolution (time-scale on the order of years) has been done on the basis of this work. However, not many analytical approaches have been published, probably because of their limited applicability for describing the finer details of shoreline change. Contributors in this field include Bakker and Edelman (1965), Bakker (1969), Bakker, Klein-Breteler, and Roos (1971), Bakker (1970), Grijm (1961, 1965), Le Méhauté and Brebner (1961), Le Méhauté and Soldate (1977, 1978, 1979), and Walton and Chiu (1979).

#### One-Line Theory

4. The aim of the one-line theory is to describe long-term variations in shoreline position. Short-term variations (e.g., changes caused by storms or by rip currents) are regarded as negligible perturbations superimposed on the main trend of shoreline evolution. In the one-line theory, the beach profile is assumed to maintain an equilibrium shape, implying that all bottom contours are parallel. Consequently, under this assumption it is sufficient to consider the movement of one line in studying the shoreline change, and that line is conveniently taken to be the shoreline, which is easily observed (Figure 1).

5. In the model, longshore sand transport is assumed to occur uniformly over the whole beach profile down to a certain critical depth  $D$  called the depth of closure. No sand is presumed to move alongshore in the region seaward of this depth. If the beach profile moves only parallel to itself (maintaining its shape), a change in shoreline position  $\Delta y$  at a certain point is related to the change in cross-sectional area  $\Delta A$  at the same point according to Equation 1:

$$\Delta A = \Delta y D \quad (1)$$

where

$\Delta A$  = change in cross-sectional beach area ( $m^2$ )

$\Delta y$  = change in shoreline position (m)

$D$  = maximum depth for sand motion (depth of closure) (m)

6. The principle of mass conservation must apply to the system at all times. By considering a control volume of sand and formulating a mass balance during an infinitesimal interval of time, the following differential equation is obtained (see Figure 1):

$$\frac{\partial Q}{\partial x} + \frac{\partial A}{\partial t} = 0 \quad (2)$$

where

$Q$  = longshore sand transport rate ( $m^3/\text{sec}$ )

$A$  = cross-sectional area of the beach ( $m^2$ )

$x$  = space coordinate along the axis parallel to the trend of the shoreline (m)

$t$  = time (sec)

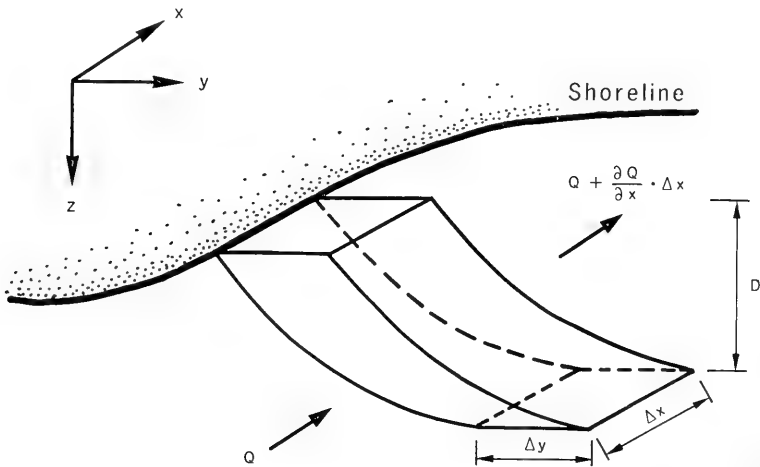


Figure 1. Schematic illustration of a hypothetical equilibrium beach profile

7. Equation 2 states that the longshore variation in the sand transport rate is balanced by changes in the shoreline position. If, in addition to longshore transport, a line source or sink of sand at the shoreline is considered, Equation 2 takes the following form:

$$\frac{\partial Q}{\partial x} + \frac{\partial A}{\partial t} = \pm q \quad (3)$$

where  $q$  denotes the source or sink of sand per unit length of beach ( $m^3/m/sec$ ). The minus sign denotes a sink (loss of sand), and the plus sign denotes a source.

8. In order to solve Equation 2, it is necessary to specify an expression for the longshore sand transport rate. Longshore sand transport on an open coast is believed to bear a close relation to the longshore current which is generated by waves obliquely incident to the shoreline. A general expression for the longshore transport rate is

$$Q = Q_o \sin 2\alpha_b \quad (4)$$

where

$Q_o$  = amplitude of longshore sand transport rate ( $m^3/sec$ )

$\alpha_b$  = angle between breaking wave crests and shoreline

In the generally accepted formula for longshore current, the speed of the current is proportional to  $\sin 2\alpha_b$  (Longuet-Higgins 1970a,b).

9. The angle between the breaking wave crests and the shoreline (Figure 2) may be expressed as

$$\alpha_b = \alpha_o - \arctan \left( \frac{\partial y}{\partial x} \right) \quad (5)$$

in which

$\alpha_o$  = angle of breaking wave crests relative to an axis set parallel to the trend of the shoreline

$\partial y/\partial x$  = local shoreline orientation

10. A wide range of expressions exists for the amplitude of the longshore sand transport rate, mainly based on empirical results. For example, the Shore Protection Manual (SPM) (1984) gives the following equation:

$$Q_o = \frac{\rho g}{16} H_{sb}^2 C_{g_b} \frac{K}{(\rho_s - \rho)\lambda} \quad (6)$$

where

- $\rho$  = density of water ( $\text{kg/m}^3$ )
- $g$  = acceleration of gravity ( $\text{m/sec}^2$ )
- $H_{sb}$  = significant breaking wave height (m)
- $Cg_b$  = wave group velocity at breaking point (m/sec)
- $K$  = nondimensional empirical constant
- $\rho_s$  = density of sand ( $\text{kg/m}^3$ )
- $\lambda$  = porosity of sand

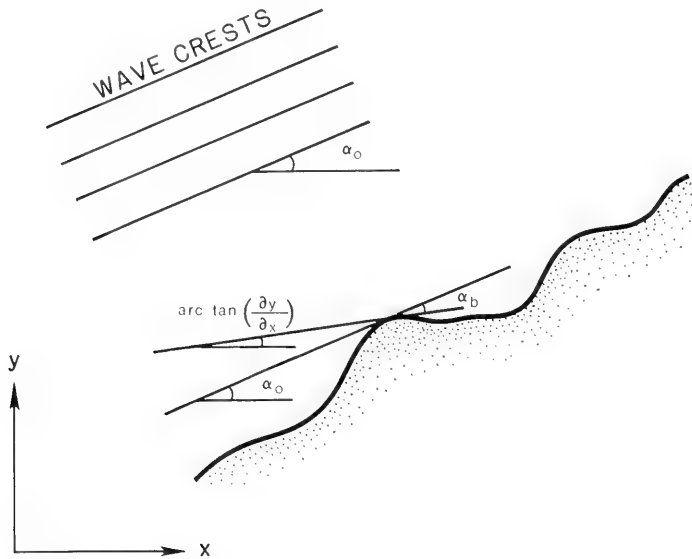


Figure 2. Definition sketch for geometric properties at a specific location as related to shoreline change

11. If Equation 5 is substituted into Equation 4, the sand transport rate can be written:

$$Q = Q_0 \sin \left\{ 2 \left[ \alpha_0 - \text{arc tan} \left( \frac{\partial y}{\partial x} \right) \right] \right\} \quad (7)$$

12. For beaches with mild slopes, it can safely be assumed that the breaking wave angle relative to the shoreline and the shoreline orientation are small. The consequences and validity of this assumption, which linearizes Equation 7, are discussed further in this report. Under the assumption of small angles, to first order in a Taylor series,

$$Q = Q_0 \left( 2\alpha_0 - 2 \frac{\partial y}{\partial x} \right) \quad (8)$$

13. If the amplitude of the longshore sand transport rate and the incident breaking wave angle are constant (independent of  $x$  and  $t$ ) the following equation may be derived from Equations 1, 2, and 8:

$$\epsilon \frac{\partial^2 y}{\partial x^2} = \frac{\partial y}{\partial t} \quad (9)$$

where

$$\epsilon = \frac{2Q_0}{D} \quad (10)$$

14. Equation 9 is formally identical to the one-dimensional equation describing conduction of heat in solids or the diffusion equation. Thus, many analytical solutions can be found by applying the proper analogies between initial and boundary conditions for shoreline evolution and the processes of heat conduction and diffusion. The coefficient  $\epsilon$ , having the dimensions of length squared over time, is interpreted as a diffusion coefficient expressing the time scale of shoreline change following a disturbance (wave action). A high amplitude of the longshore sand transport rate produces a rapid shoreline response to achieve a new state of equilibrium with the incident waves. Furthermore, a larger depth of closure indicates that a larger part of the beach profile participates in the sand movement, leading to a slower shoreline response.

15. If the amplitude of the longshore sand transport rate is a function of  $x$ , the governing differential equation for the shoreline position will take a different form:

$$\epsilon \frac{\partial^2 y}{\partial x^2} + \frac{d\epsilon}{dx} \frac{\partial y}{\partial x} = \alpha_0 \frac{d\epsilon}{dx} + \frac{\partial y}{\partial t} \quad (11)$$

where it is assumed that the depth of closure is constant. Equation 11 makes it possible, in a simplified way, to account for diffraction behind a groin, where the wave height varies with distance alongshore. However, the

expression describing the variation in  $Q_0$  in a diffraction zone must be simple enough to allow an analytical solution. Otherwise, a numerical solution technique must be employed (Kraus and Harikai 1983, Kraus 1983, and Hanson and Kraus 1986). If the incident breaking wave angle  $\alpha_0$  is also a function of the distance  $x$ , another term,  $\varepsilon d\alpha_0/dx$ , must be added to the right side of Equation 11.

16. In summary, the assumptions which comprise the one-line model, in which breaking waves are the dominant sand-moving process, are as follows:

- a. The beach profile moves parallel to itself (assumption of equilibrium of the beach profile).
- b. Longshore sand transport takes place uniformly over the beach profile down to a depth  $D$  (depth of closure).
- c. Details of the nearshore circulation are neglected.
- d. The longshore sand transport rate is proportional to the angle of incidence of breaking wave crests to the shoreline.

17. In addition, the following assumptions will be used to derive analytical (closed-form) solutions of the one-line model (Equation 9):

- a. The angle between the breaking wave crests and the shoreline is small (small-angle approximation).
- b. The angle of the shoreline with respect to the  $x$ -axis is small.

18. In arriving at all solutions, it is tacitly assumed that sand is always available for transport unless explicitly restricted by boundary and/or initial conditions.

### Overview of Previous Analytical Work

19. Pelnard-Considère (1956) was the first to employ mathematical modeling as a method of describing shoreline evolution. He introduced the one-line theory and verified its applicability with laboratory experiments. Figure 3 shows a comparison between experimental results and the analytical solution for the case of an updrift groin, as obtained by Pelnard-Considère. Pelnard-Considère derived analytical solutions of Equation 9, the linearized shoreline change equation, for three different boundary conditions: shoreline evolution updrift of a groin (with and without bypassing) and release of an instantaneous plane source of sand on the beach.

20. Grijm (1961) studied delta formation from rivers discharging sand. In the transport equation discussed in his article, the sand transport rate



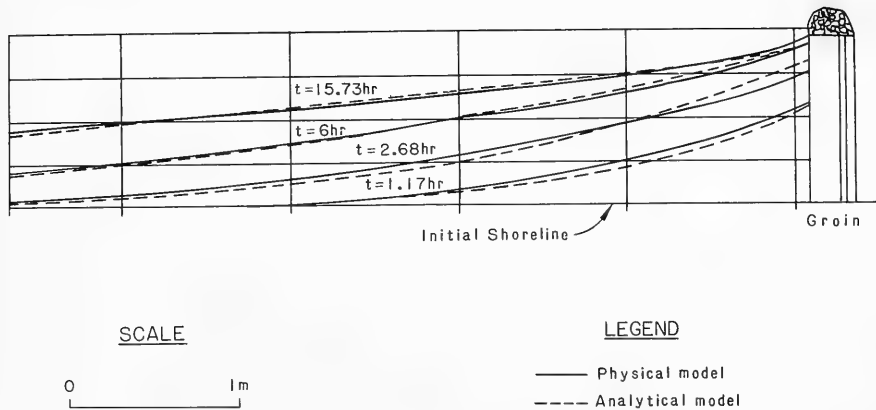


Figure 3. Comparison between experimental and theoretical shoreline evolution (after Pelnard-Considère 1956)

is set to be proportional to twice the incident breaking wave angle to the shoreline. Only solutions which were similar in shape during the course of time are discussed. Two different analytical solutions are presented: one for which the incident breaking wave angle and the shoreline orientation angle are small and one for which the wave angle is small in comparison with the shoreline orientation. The governing equations (sand transport and mass conservation) are expressed in polar coordinates and solved numerically. Grijm (1965) further develops this technique and presents a wide range of delta formations. Komar (1973) also presents numerically obtained solutions of delta growth under highly simplified conditions.

21. Le Méhauté and Brebner (1961) discuss solutions for shoreline change at groins, with and without bypassing of sand, and the effect of sudden dumping of material at a given point. Most of the solutions were previously derived by Pelnard-Considère (1956), but they are more thoroughly presented in Le Méhauté and Brebner's work, especially regarding geometric aspects of the shoreline change. The decay of an undulating shoreline and the equilibrium shape of the shoreline between two headlands are treated.

22. Bakker and Edelman (1965) modify the longshore sand transport rate equation to allow for an analytical treatment without linearization. The sand transport rate is divided into two different cases:

$$Q = Q_o K_1 \tan \alpha_b \quad 0 \leq \tan \alpha_b \leq 1.23 \quad (12)$$

$$Q = Q_o \frac{K_2}{\tan \alpha_b} \quad 1.23 < \tan \alpha_b \quad (13)$$

where  $K_1$  and  $K_2$  are constants. From these equations as a starting point, the growth of river deltas was studied.

23. Bakker (1969) extends the one-line theory to include two lines to describe beach planform change. The beach profile is divided into two parts, one relating to shoreline movement and one to movement of an offshore contour (see Figure 4). The two-line theory provides a better description of sand

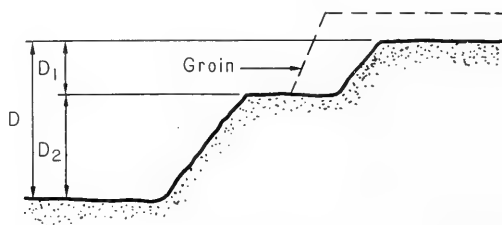


Figure 4. Definition sketch for the two-line theory (after Bakker 1968)

movement downdrift of a long groyne since it describes representative changes in the contours seaward of the groyne head. Near structures such as groynes, offshore contours may have a different shape from the shoreline. The two lines in the model are represented by a system of two differential equations which are coupled through a term describing cross-shore transport. According to Bakker (1969), the cross-shore transport rate depends on the steepness of the beach profile; a steep profile implies offshore sand transport; and gently sloping profile implies onshore sand transport. Analytical solutions of the two-line theory are not included in the present report. However, an example of a two-line theory solution for a groyne system is shown in Figure 5. The solution describes the stationary form of the shoreline for various groyne spacings given in multiples of a nondimensional groyne length  $L_o$ .

24. The two-line theory is further developed in Bakker, Klein-Breteler, and Roos (1971) in which diffraction behind a groyne is treated. In this case, it became necessary to numerically solve the governing equations. Expressions for the coastal constant (diffusion coefficient  $\epsilon$ ) for the one- and two-line

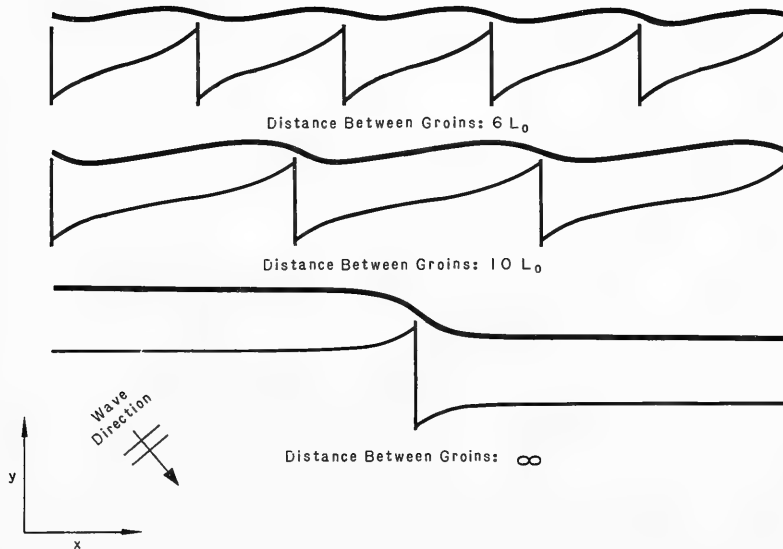


Figure 5. Two-line theory solution for a groin system  
(after Bakker 1968)

theories are also presented. Bakker (1970) developed a phenomenological diffraction routine for one-line theory but numerically solved the problem.

25. Le Méhauté and Soldate (1977) present a brief literature survey on the subject of mathematical modeling of shoreline evolution. Analytical solutions of the linearized shoreline change equation are discussed together with the spread of a rectangular beach fill. In Le Méhauté and Soldate (1978, 1979) a numerical model is derived which includes variation in sea level, wave refraction and diffraction, rip currents, and the effects of coastal structures in connection with long-term shoreline evolution.

26. Until recently, the most complete summary of analytical solutions to the sand transport equation has been made by Walton and Chiu (1979). Two derivations of the linearized shoreline change equation are presented together with another approach resulting in a nonlinear model. The difference between the two approaches, which both arrive at the diffusion equation, is that one uses the Coastal Engineering Research Center (CERC) formula (SPM 1984, Chapter 4) for describing the longshore sand transport rate by wave action and the

other a formula derived by Dean (1973) based on the assumption that the major sand transport occurs as suspended load. Most analytical solutions then appearing in the literature were presented by Walton and Chiu (1979). Additional solutions mainly concern beach nourishment in connection with various shoreline shapes. The new solutions derived by Walton and Chiu (1979) treat beach fill in a triangular shape, a rectangular gap in a beach, and a semi-infinite rectangular fill. Some data on the coastal constant are also presented in the paper.

27. Analytical solutions can be used conveniently to describe the behavior of beach fill, as mentioned above. Dean (1984) gives a brief survey of some solutions applicable to beach nourishment calculations, especially in the form of characteristic quantities describing loss percentages. One solution describes the shoreline change between two groins initially filled with sand. The resultant shoreline evolution with time is shown in Figure 6.

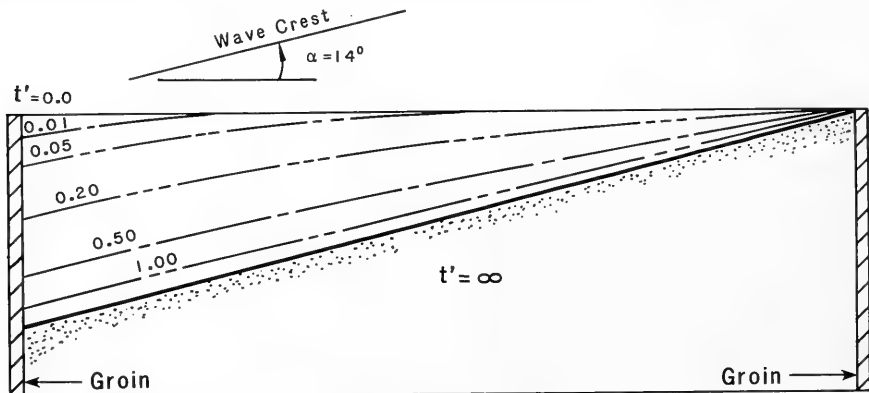


Figure 6. Shoreline evolution between two groins initially filled with sand (after Dean 1984)

#### General Approach in the Present Work

28. The simplified or linearized shoreline change equation (Equation 9) is a linear partial differential equation which is identical to the equation describing one-dimensional conduction of heat in a solid or to the diffusion equation. By specifying boundary and initial conditions in these areas which represent conditions prevailing in a specific shoreline evolution situation, the corresponding analytical solutions are directly applicable. Carslaw and

Jaeger provide many solutions of the heat conduction equation, and Crank (1975) gives solutions to the diffusion equation.

29. The following paragraphs present a review of previously obtained solutions together with new solutions. The new solutions have been derived either from analogies with heat conduction or through the Laplace transform technique, a short outline for which is given in Appendix A. Carslaw and Jaeger (1959) provide a more comprehensive treatment. In order to present the solutions in an efficient and general format dimensionless variables have been used to a large extent although physical understanding may be obscured by the absence of dimensional quantities. Also, in many cases for which the solution is symmetric with respect to a coordinate axis, the solution for only one side of the symmetry line is displayed. The solutions have been divided into two groups based on the physical properties of the initial and boundary conditions, not on their mathematical properties, because the object of the report is to present solutions and not to describe details of their derivation. The first group of solutions describes shoreline change situations without coastal structures. Solutions describing shoreline evolution in these cases are applicable both to natural and artificial beach forms (nourished beaches) if similar types of wave conditions prevail. Also, several solutions describing river delta growth are presented covering the cases of a river discharging sand as a point source and a river mouth of finite length.

30. The other group of solutions comprises configurations involving various types of coastal structures such as groins, jetties, detached breakwaters, and seawalls. Since the equations quickly become complicated, the influence of coastal structures on shoreline evolution has to be idealized to a considerable extent. However, the essential features of the situation may still be preserved if this idealization is carried out in a physically reasonable manner. Some simple models to account for diffraction downdrift of a groin are shown also.

31. Most of the analytical solutions are presented in the main text without derivation. Reference is made to the appropriate literature in case the reader is interested in deriving the solutions. Also, in Appendixes B-G, derivations are given for selected new solutions.

PART II: SOLUTIONS FOR SHORELINE EVOLUTION WITHOUT  
COASTAL STRUCTURES

General Formal Solution

32. The basic differential equation to solve is Equation 9, together with the associated initial and boundary conditions. An infinitely long beach is assumed to be exposed to waves of constant height and period with wave crests parallel to the x-axis (parallel to the trend of the shoreline). The shoreline will adjust to reach an equilibrium state in which the longshore sand transport rate is equal at every point along the shoreline. Since the wave crests are parallel to the x-axis, the equilibrium sand transport rate is zero. An initially straight beach is thus the stable shoreline form in this case. If the shoreline shape at time  $t = 0$  is described by a function  $f(x)$ , the solution of Equation 9 is given by the following integral (Carslaw and Jaeger 1959, p. 53):

$$y(x,t) = \frac{1}{2\sqrt{\pi\epsilon t}} \int_{-\infty}^{\infty} f(\xi) e^{-(x-\xi)^2/4\epsilon t} d\xi \quad (14)$$

for  $t > 0$  and  $-\infty < x < \infty$ .

The shoreline position is denoted by  $y$  and is a function of  $x$  and  $t$ . The quantity  $\xi$  is a dummy integration variable. Consequently, the change in both natural and manipulated beach forms can be determined if Equation 14 is evaluated. Equation 14 may be interpreted as a superposition of an infinite number of plane sources instantaneously released at  $t = 0$ . The source located at point  $\xi$  contributes an amount  $f(\xi)d\xi$  to the system. Infinitely far away from such a single source no effect on the shoreline position is assumed (boundary condition). Equation 14 is used to derive most of the solutions dealing with various shoreline configurations in the following text.

### Finite Rectangular Beach Fill

33. The solution to this problem in connection with shoreline change is first mentioned by Le Méhauté and Soldate (1977). At time  $t = 0$ , the shoreline has a rectangular shape of finite length  $2a$  described by Equation 15 (see Figure 7):

$$y(x,0) = f(x) = \begin{cases} y_0 & |x| \leq a \\ 0 & |x| > a \end{cases} \quad (15)$$

The solution is

$$y(x,t) = \frac{1}{2} y_0 \left[ \operatorname{erf} \left( \frac{a-x}{2\sqrt{\epsilon t}} \right) + \operatorname{erf} \left( \frac{a+x}{2\sqrt{\epsilon t}} \right) \right] \quad (16)$$

for  $t > 0$  and  $-\infty < x < \infty$ .

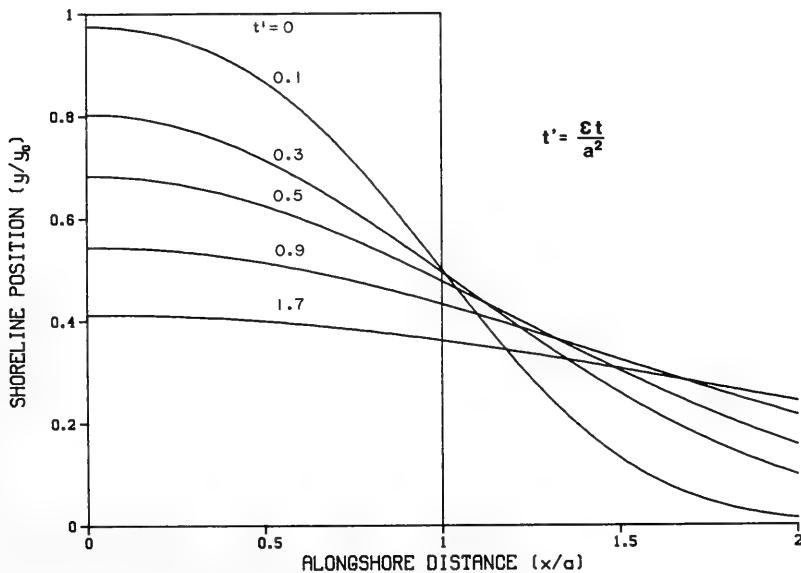


Figure 7. Shoreline evolution of an initially rectangular beach fill exposed to waves arriving normal to shore

The symbol  $\text{erf}$  denotes the error function which is defined as

$$\text{erf } z = \frac{2}{\sqrt{\pi}} \int_0^z e^{-\xi^2} d\xi \quad (17)$$

The error function is tabulated in standard mathematical reference books (e.g., Abramowitz and Stegun 1965). It is convenient to introduce the following dimensionless quantities:

$$y' = \frac{y}{y_0} \quad (18)$$

$$x' = \frac{x}{a} \quad (19)$$

$$t' = \frac{\epsilon t}{a^2} \quad (20)$$

The quantity used to normalize the time variable expresses half the time elapsed before a square beach fill of length  $a$  would completely erode at the constant transport rate  $Q_0$ . If the solution is expressed in dimensionless quantities, the resultant shoreline evolution can be displayed in compact form. Figure 7 illustrates how a rectangular fill spreads or diminishes with time according to Equation 16. It should be noted that the vertical scale of this and the following figures has been distorted for the sake of clarity.

34. Dean (1984) discusses how the sand from two different beach nourishment projects spreads with time. The time  $t_{P2}$  for a certain percentage  $P$  to be lost from the original rectangular beach fill is compared with the corresponding time  $t_{P1}$  for different conditions:

$$t_{P2} = t_{P1} \left( \frac{a_2}{a_1} \right)^2 \frac{\epsilon_1}{\epsilon_2} \quad (21)$$

35. This formula is obtained by noting that the same percentage of beach volume is lost during the same dimensionless time. Consequently, a



rectangular beach fill which is twice as long maintains its volume four times as long if exposed to the same wave conditions. It is possible to calculate the time it will take for a certain percentage  $P$  to be lost from the initial rectangular fill. The following expression is obtained by integrating Equation 16 and comparing the resulting volume at a specific time to the original fill volume:

$$P = \sqrt{t^*} \left( \frac{1}{\sqrt{\pi}} - \text{ierfc} \frac{1}{\sqrt{t^*}} \right) \quad (22)$$

where  $\text{ierfc}$  denotes the integral of the complementary error function  $\text{erfc}$  :

$$\text{ierfc} z = \int_z^{\infty} \text{erfc} \xi \, d\xi \quad (23)$$

$$\text{erfc} z = 1 - \text{erf} z \quad (24)$$

Figure 8 shows the percentage of sand volume lost as a function of time.

36. It is possible to determine the rate of sand to be supplied to the fill in order to maintain the original shape. The boundary condition for this case is that the end of the rectangular fill is kept at the initial position:

$$y(0,t) = y_0 \quad (25)$$

Note in this case that the  $x$ -axis originates from the corner of the fill instead of from the middle of the fill as in Equation 16. The solution describing the resultant shoreline evolution is (Carslaw and Jaeger 1959, p. 60):

$$y(x,t) = y_0 \text{erfc} \left( \frac{x}{2\sqrt{\epsilon t}} \right) \quad (26)$$

for  $t > 0$  and  $x \geq 0$ .

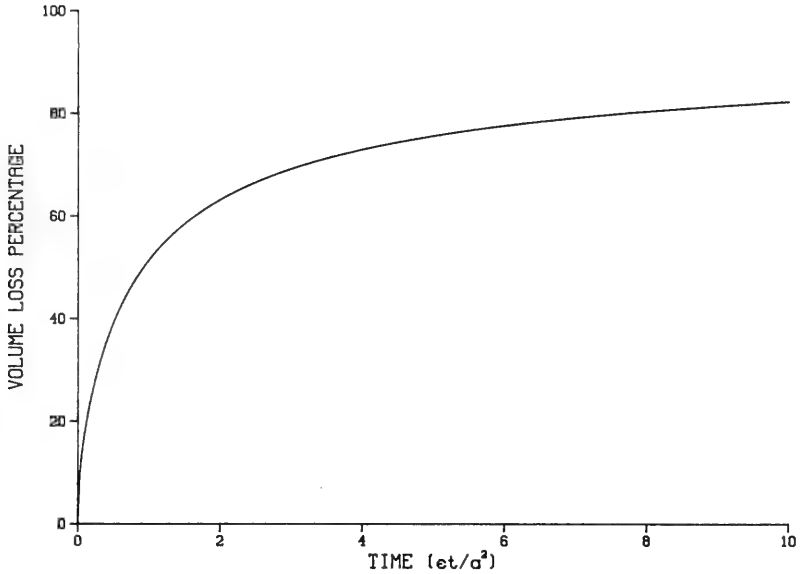


Figure 8. Percentage of sand volume lost from a rectangular fill as a function of dimensionless time

Sand has to be added to the corner of the fill at the following rate:

$$Q = \frac{2y_0}{\sqrt{\pi\epsilon t}} Q_0 \quad (27)$$

The spread of the moving shoreline front (Equation 26) is illustrated in Figure 9.

37. It is advisable to use the analytical expressions describing shoreline evolution for a rectangular fill with great care, even for rough estimations, because the linearization procedure (Equation 8) is based on small shoreline orientation angles, a condition which is violated on the sides of the rectangle. In fact, the linearized transport equation implies an infinitely large initial sand transport rate at the edges of the fill. However, the original transport equation (Equation 7) gives a zero transport rate at the corners; thus, a rectangular beach form is stable to parallel incident waves. In reality, sand transport occurs at the corners because of

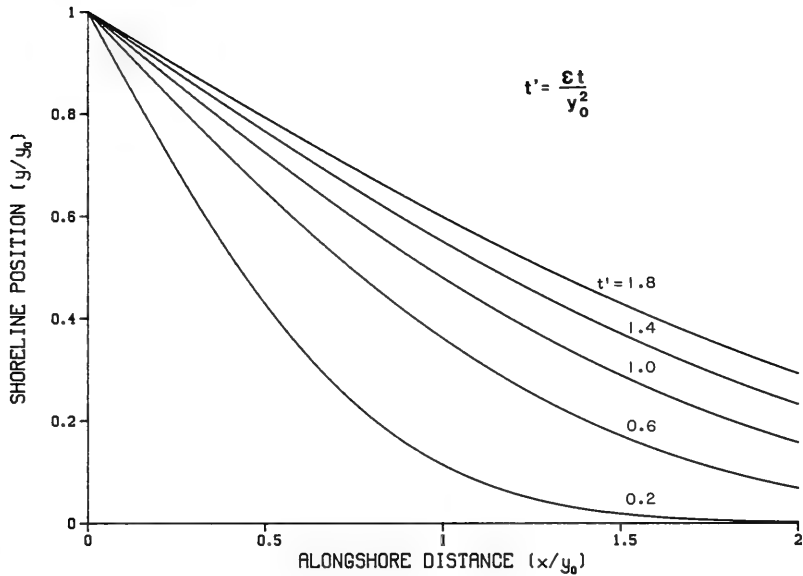


Figure 9. Shoreline evolution when sand is supplied at  $x = 0$  to maintain a specific beach width  $y_0$

diffraction and refraction, but this realistic situation is not described by the linearized equation. Consequently, the linearization procedure artificially increases the erosion of the fill, implying that the analytical solution overestimates the speed of erosion. The error is, therefore, on the conservative side. This problem is only an apparent one since it is a practical impossibility to create a perfectly rectangular fill in the field.

#### Semi-Infinite Rectangular Beach Fill

38. The initial conditions for a semi-infinite rectangular beach fill are

$$y(x,0) = \begin{cases} y_0 & x \leq 0 \\ 0 & x > 0 \end{cases} \quad (28)$$

Walton and Chiu (1979) give the following solution:

$$y(x,t) = \frac{1}{2} y_0 \operatorname{erfc} \left( \frac{x}{2\sqrt{\epsilon t}} \right) \quad (29)$$

for  $t > 0$  and  $-\infty < x < \infty$ .

The solution is antisymmetric about the  $y$ -axis, taking the constant value  $y_0/2$  at  $x = 0$ . If the shape of the shoreline for  $x \geq 0$  is approximated by a triangle having height  $y_0/2$  so as to conserve mass, the speed of propagation of the triangle's front is inversely proportional to the square root of elapsed time. This relationship is also valid for Equation 26. Figure 10 illustrates the solution of Equation 29. The right side of Equation 29 for  $x > 0$  equals half the solution of Equation 26.

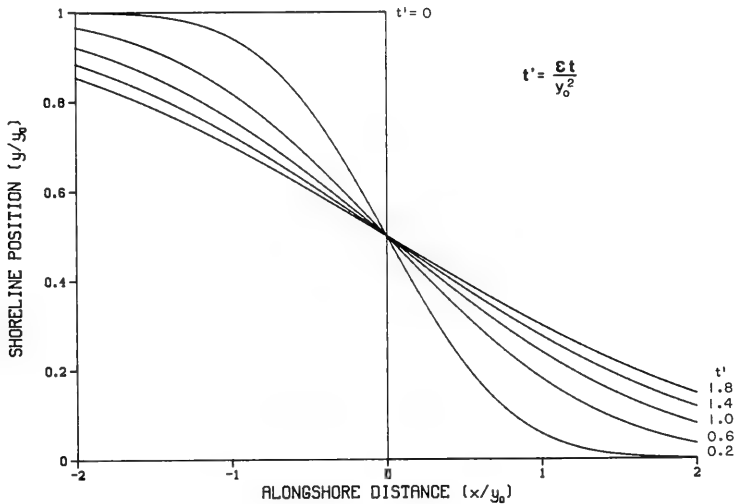


Figure 10. Shoreline evolution of an initially semi-infinite rectangular beach

#### Rectangular Cut in a Beach

39. The initial conditions for rectangular cut in a beach are formulated as

$$y(x,0) = \begin{cases} y_0 & |x| \geq a \\ 0 & |x| < a \end{cases} \quad (30)$$

These conditions may represent an excavation or a natural embayment of rectangular shape. Walton and Chiu (1979) present the following solution:

$$y(x,t) = \frac{1}{2} y_0 \left[ \operatorname{erfc} \left( \frac{a-x}{2\sqrt{\epsilon t}} \right) + \operatorname{erfc} \left( \frac{a+x}{2\sqrt{\epsilon t}} \right) \right] \quad (31)$$

for  $t > 0$  and  $-\infty < x < \infty$ .

This solution may be obtained by superimposing Equation 16 with a negative sign on a beach of width  $y_0$ . In general, with due regard to the boundary and initial conditions, it is possible to derive new solutions simply by superimposing existing solutions since the governing differential equation (Equation 9) is linear. Equation 31 is symmetric with respect to the  $y$ -axis, and only half of the solution region is illustrated in Figure 11.

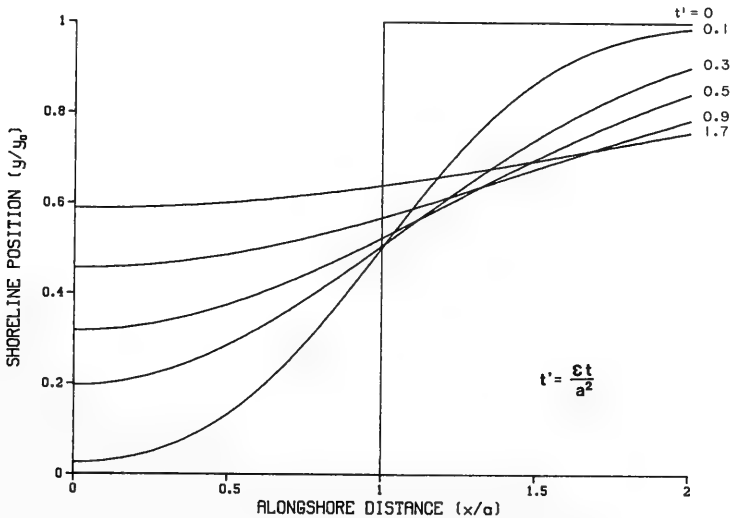


Figure 11. Shoreline evolution of a rectangular cut in an infinite beach of width  $y_0$

40. Since the present situation is the inverse problem of the rectangular beach fill, Figure 8 can be used to evaluate the rate of infilling of a certain volumetric percentage of sand.

#### Triangular-Shaped Beach

41. The triangular-shaped solution is also mentioned by Walton and Chiu (1979). The original beach has the shape of a triangle according to the initial conditions as follows:

$$y(x,0) = \begin{cases} y_0 \left( \frac{a-x}{a} \right) & 0 \leq x \leq a \\ y_0 \left( \frac{a+x}{a} \right) & -a \leq x \leq 0 \\ 0 & |x| > a \end{cases} \quad (32)$$

In this case the solution takes the following form:

$$y(x,t) = \frac{y_0}{2a} \left\{ (a-x) \operatorname{erf} \left( \frac{a-x}{2\sqrt{\epsilon t}} \right) + (a+x) \operatorname{erf} \left( \frac{a+x}{2\sqrt{\epsilon t}} \right) - 2x \operatorname{erf} \left( \frac{x}{2\sqrt{\epsilon t}} \right) + 2 \sqrt{\frac{\epsilon t}{\pi}} \left[ e^{-(x+a)^2/4\epsilon t} + e^{-(x-a)^2/4\epsilon t} - 2e^{-x^2/4\epsilon t} \right] \right\} \quad (33)$$

for  $t > 0$  and  $-\infty < x < \infty$ .

A nondimensional illustration of the shoreline evolution from an initially triangular beach is shown in Figure 12.

42. Depending upon the height-to-width ratio of the triangle, linearization of the transport equation may reduce accuracy of the analytical solution. However, even though the assumptions forming the basis for the linearization procedure appear to be extremely limiting (particularly in requiring small wave angles), in practice the analytical solution is found to be applicable for angles as large as about 45 deg between the shoreline and the breaking waves. In order to estimate the effect of the linearization, a comparison

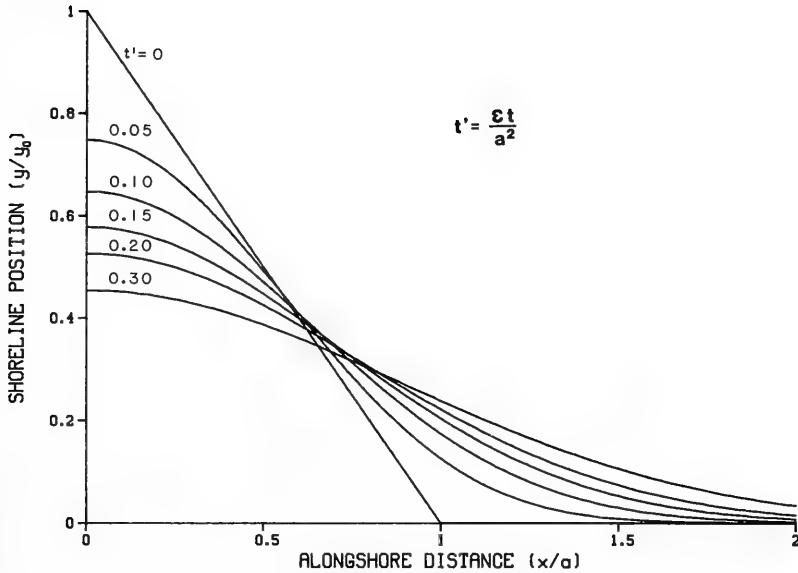


Figure 12. Shoreline evolution of an initially triangular beach was made between the analytical solution and a numerical solution with the original sand transport equation (Equation 7). Figure 13 shows the result as a function of the height-to-width ratio and elapsed time.

43. It is quite clear that the analytical solution produces a higher rate of shoreline change by overestimating the longshore sand transport rate (since  $\alpha > \sin \alpha$ ). Thus, if the analytical solution is used to estimate the time scale involved in beach nourishment problems, a higher rate of attenuation of the fill will always be obtained than is expected to actually occur.

#### Trapezoidal-Shaped Beach

44. A trapezoidal beach form is described by the following initial conditions:

$$y(x,0) = \begin{cases} \frac{y_2 - y_1}{x_2 - x_1} x + \frac{y_1 x_2 - x_1 y_2}{x_2 - x_1} & x_1 \leq x \leq x_2 \\ 0 & x < x_1, \quad x > x_2 \end{cases} \quad (34)$$

Here  $y_1$  and  $y_2$  denote shoreline positions corresponding to the longshore locations  $x_1$  and  $x_2$ . The solution is

$$y(x,t) = \frac{1}{2} \left( \frac{y_2 - y_1}{x_2 - x_1} x + \frac{y_1 x_2 - x_1 y_2}{x_2 - x_1} \right) \left[ \operatorname{erf} \left( \frac{x_2 - x}{2\sqrt{\epsilon t}} \right) - \operatorname{erf} \left( \frac{x_1 - x}{2\sqrt{\epsilon t}} \right) \right] + \left( \frac{y_2 - y_1}{x_2 - x_1} \right) \sqrt{\frac{\epsilon t}{\pi}} \left[ e^{-\frac{(x_1 - x)^2}{4\epsilon t}} - e^{-\frac{(x_2 - x)^2}{4\epsilon t}} \right] \quad (35)$$

for  $t > 0$  and  $-\infty < x < \infty$ .

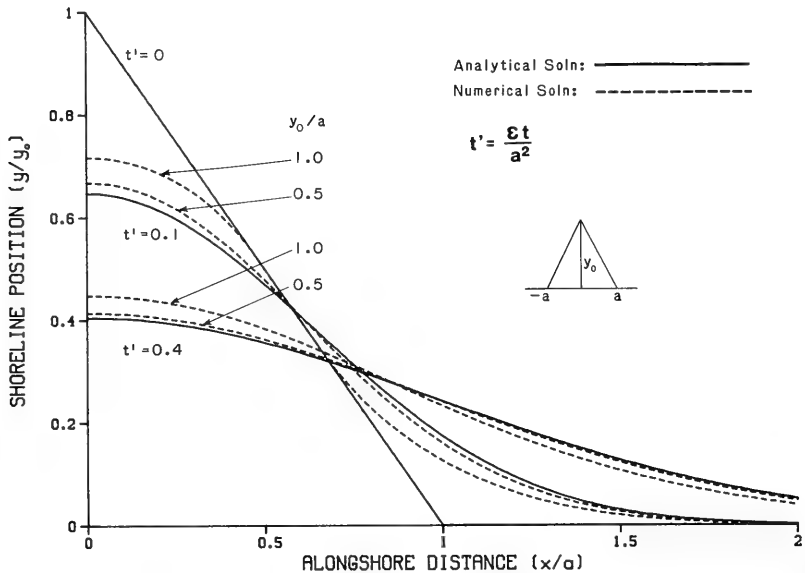


Figure 13. Comparison between analytical solution with the linearized transport equation and numerical solution with the original transport equation for a triangular beach fill (for height-to-width ratios 1.0 and 0.5)

The solution for the triangular beach form (Equation 33) can be obtained by superimposing two trapezoidal beach shapes which reduce to triangles. In the same way, in principle, the analytical solution for any arbitrary shoreline shape may be obtained by approximating the shoreline with a series of straight lines. Even though the sand transport at each boundary of the trapezoids in



such a case is overestimated (because of the large incident wave angle) superimposition of the solutions eliminates these effects. In Figure 14 the solution for a single trapezoidal beach form is shown. A representative length  $L$  has been chosen to normalize the shoreline position and the alongshore distance.

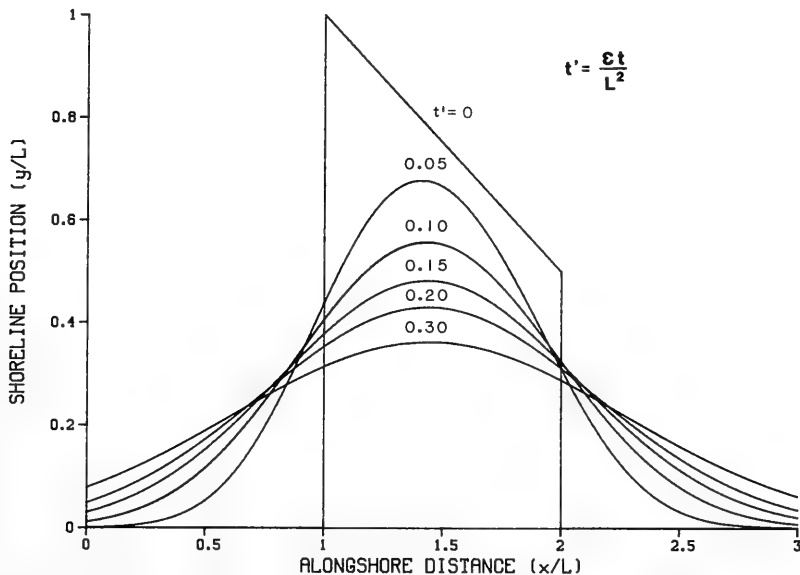


Figure 14. Shoreline evolution of an initially trapezoidal beach form

45. If an arbitrary-shaped shoreline is studied, it is most convenient to approximate it with a series of straight lines and then to superimpose the respective solutions. Consider a shoreline (see Figure 15) divided into  $N$  reaches, with each length described by a straight line connecting two neighboring points denoted by  $(x_i, y_i)$  and  $(x_{i+1}, y_{i+1})$  for a certain reach (the  $i^{\text{th}}$  reach).

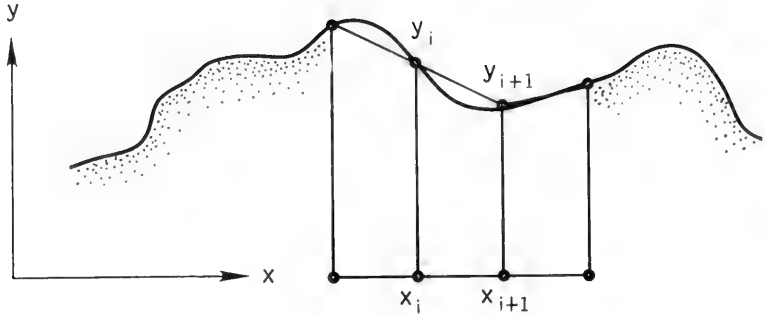


Figure 15. Shoreline of arbitrary shape approximated by  $N$  straight lines

46. The shoreline position can be written, accordingly:

$$y(x,t) = \frac{1}{2} \sum_{i=1}^N \left\{ \left( \frac{y_{i+1} - y_i}{x_{i+1} - x_i} x + \frac{y_i x_{i+1} - x_i y_{i+1}}{x_{i+1} - x_i} \right) \left[ \operatorname{erf} \left( \frac{x - x_i}{2\sqrt{\epsilon t}} \right) - \operatorname{erf} \left( \frac{x - x_{i+1}}{2\sqrt{\epsilon t}} \right) \right] + \left( \frac{y_{i+1} - y_i}{x_{i+1} - x_i} \right) 2 \sqrt{\frac{\epsilon t}{\pi}} \left[ e^{-\frac{(x-x_i)^2}{4\epsilon t}} - e^{-\frac{(x-x_{i+1})^2}{4\epsilon t}} \right] \right\} \quad (36)$$

for  $t > 0$  and  $-\infty < x < \infty$ .

#### Semicircular-Shaped Beach

47. In order to find an analytical solution for a beach formed in a half circle between  $-a < x < a$ , the circle is approximated by a polygon with a finite number of corners (Figure 16).

48. The solution can be obtained using Equation 36 with proper expressions for the line segments. The following quantities are defined:

$$x_i^R = a \cos \left[ \frac{(i-1)\pi}{N-1} \right] \quad (37)$$

$$x_i^L = a \cos \left( \frac{i\pi}{N-1} \right) \quad (38)$$

$$y_i^L = a \sin \left( \frac{i\pi}{N-1} \right) \quad (39)$$

$$k_i = \frac{1}{\tan \left[ \frac{i \left( \pi - \frac{1}{2} \right)}{N-1} \right]} \quad (40)$$

The integer  $N$  is the number of corners in the polygon approximating the semicircle. For example, if  $N = 3$  then a triangular beach form is obtained. The solution can be written with the previously defined quantities:

$$y(x,t) = \frac{1}{2} \sum_{i=1}^{N-1} \left\{ \left( k_i x_i^L + y_i^L - k_i x \right) \left[ \operatorname{erf} \left( \frac{x_i^R - x}{2\sqrt{\epsilon t}} \right) - \operatorname{erf} \left( \frac{x_i^L - x}{2\sqrt{\epsilon t}} \right) \right] + 2k_i \sqrt{\frac{\epsilon t}{\pi}} \left[ e^{-\frac{(x_i^R - x)^2}{4\epsilon t}} - e^{-\frac{(x_i^L - x)^2}{4\epsilon t}} \right] \right\} \quad (41)$$

for  $t > 0$   $-\infty < x < \infty$ .

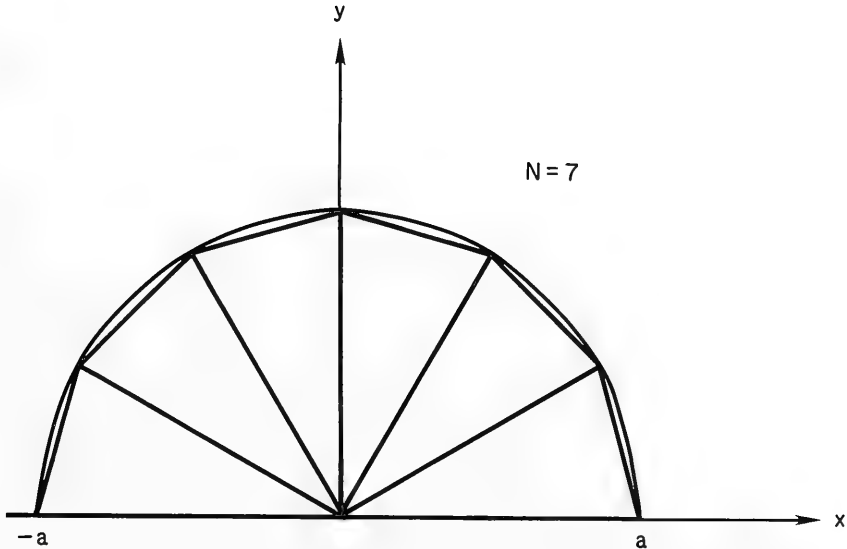


Figure 16. Semicircular-shaped beach approximated by a polygon

In the limit  $N \rightarrow \infty$  the polygon coincides with a semicircle. The solution ( $N = 101$ ) is illustrated in Figure 17 which shows the shoreline evolution as a function of time for an initially semicircular-shaped beach.

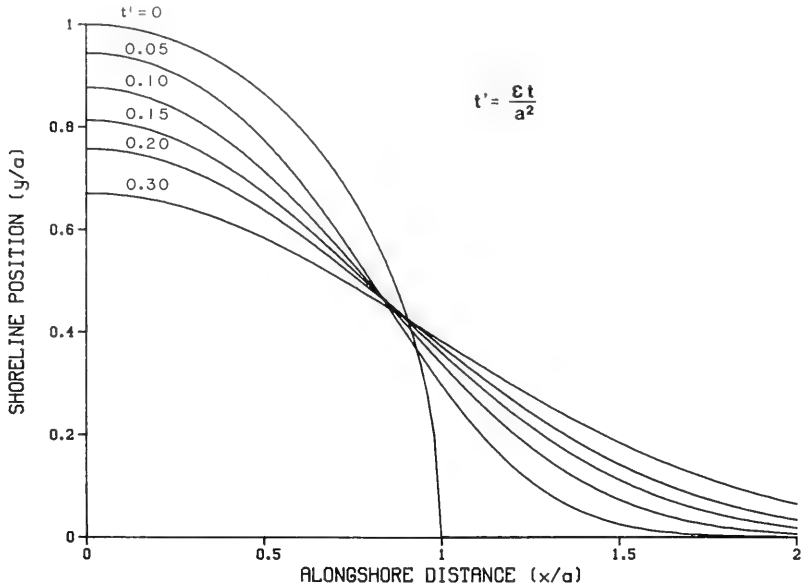


Figure 17. Shoreline evolution of an initially semicircular beach

49. If the beach is formed as a circular segment, the solution may be derived by superimposing Equation 41 with the appropriate summation limits and Equation 16 with reversed sign. In Figure 18 a definition sketch is shown. If the pitch height is denoted by  $p$ , then the width of the circle segment becomes  $2\sqrt{p(2a - p)}$ . Furthermore, the height of the rectangular fill is  $a - p$ , and the angle  $\alpha$  (see Figure 18) is  $\text{arc sin}(1 - p/a)$ . Consequently, the summation of the solutions for the polygon stretches should start at angle  $\alpha$  in the semicircle and end at angle  $\pi - \alpha$ . The solution is

$$\begin{aligned}
y(x,t) = & \frac{1}{2} \sum_{i=m+1}^{N-m-1} \left\{ y_i^L + k_i (x_i^L - x) \left[ \operatorname{erf} \left( \frac{x_i^R - x}{2\sqrt{\epsilon t}} \right) - \operatorname{erf} \left( \frac{x_i^L - x}{2\sqrt{\epsilon t}} \right) \right] \right. \\
& + 2k_i \sqrt{\frac{\epsilon t}{\pi}} \left[ e^{-\frac{(x_i^R - x)^2}{4\epsilon t}} - e^{-\frac{(x_i^L - x)^2}{4\epsilon t}} \right] \left. \right\} \\
& - \frac{1}{2} (a - p) \left[ \operatorname{erf} \left( \frac{\sqrt{p(2a - p)} - x}{2\sqrt{\epsilon t}} \right) + \operatorname{erf} \left( \frac{\sqrt{p(2a - p)} + x}{2\sqrt{\epsilon t}} \right) \right] \quad (42)
\end{aligned}$$

for  $t > 0$  and  $-\infty < x < \infty$ .

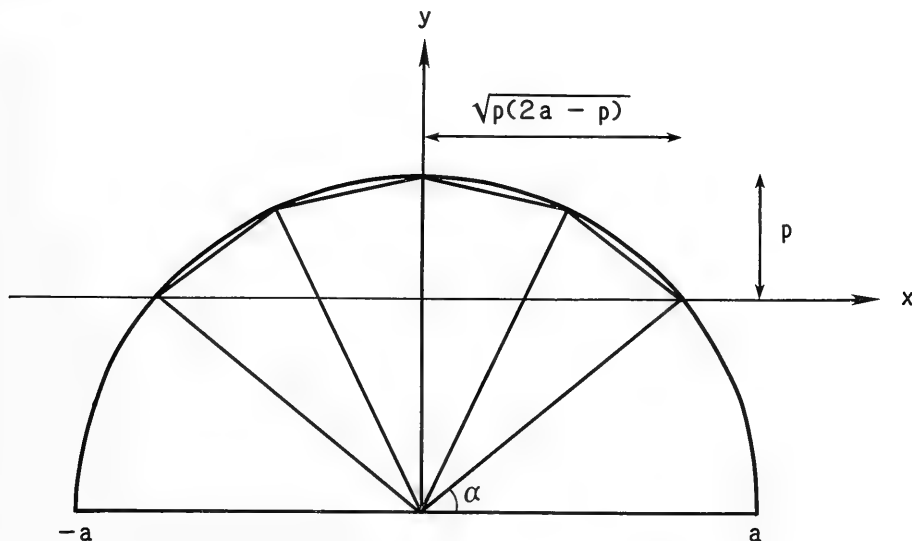


Figure 18. Definition sketch for a circular segment-shaped beach

The quantity  $N$  is, as before, the number of corners in the polygon, and  $m$  represents the number of corners minus one contained in the angle  $\alpha$ . Figure 19 illustrates the transformation of an initially circular segment-shaped shoreline.

50. Since the tangent of the shoreline orientation (see Equation 5) is infinite at the corners of the semicircle ( $x = \pm a$ ), the condition of small

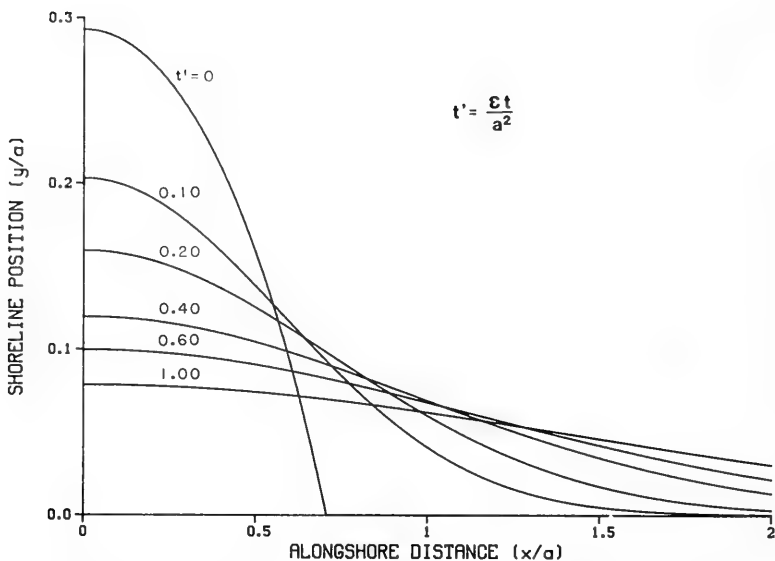


Figure 19. Shoreline evolution of an initially circular segment-shaped beach ( $\alpha = 45$  deg)

angles is violated. This condition implies, as previously discussed, that the sand transport is overestimated, leading to a faster dispersion process of the shoreline toward the stable condition (a beach parallel to the wave crests). An analytical solution for a circular segment-shaped beach, however, will show better agreement with the numerical solution of the original sand transport formula if the angle of shoreline orientation is small at the edges. A comparison between an analytical and a numerical solution for a circular segment beach is illustrated in Figure 20. In this case the linearization approximates the transport equation well; thus, the solution is accurate.

#### Semicircular Cut in a Beach

51. The situation of a semicircular cut in a beach is the antisymmetric analog of the case described in the previous section. A solution is obtained by superimposing Equation 41 with opposite sign for a beach of width  $a$ . The solution is displayed in Figure 21.

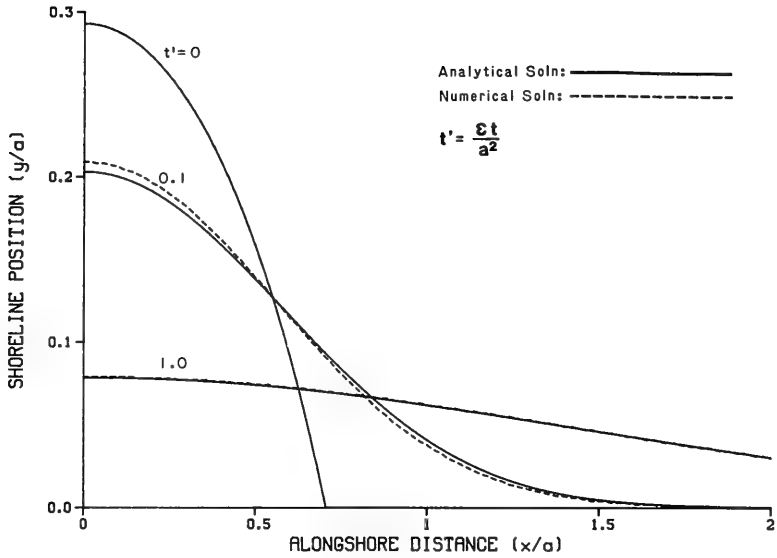


Figure 20. Comparison between analytical and numerical solutions for the case of a circular segment-shaped beach

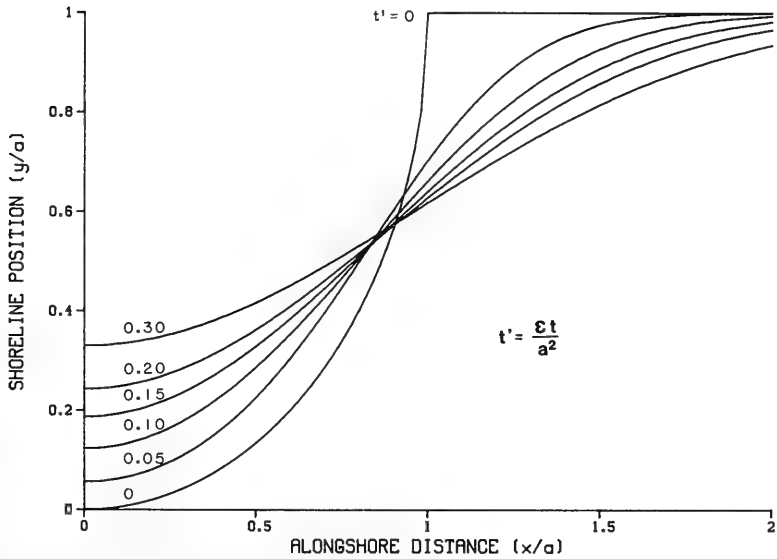


Figure 21. Shoreline evolution of an initially semicircular cut in a beach

52. In the same way, shoreline evolution of a bay formed in a circular segment may be calculated. Equation 42 is superimposed with opposite sign on a beach of width  $p$  (pitch height). Figure 22 shows the solution.

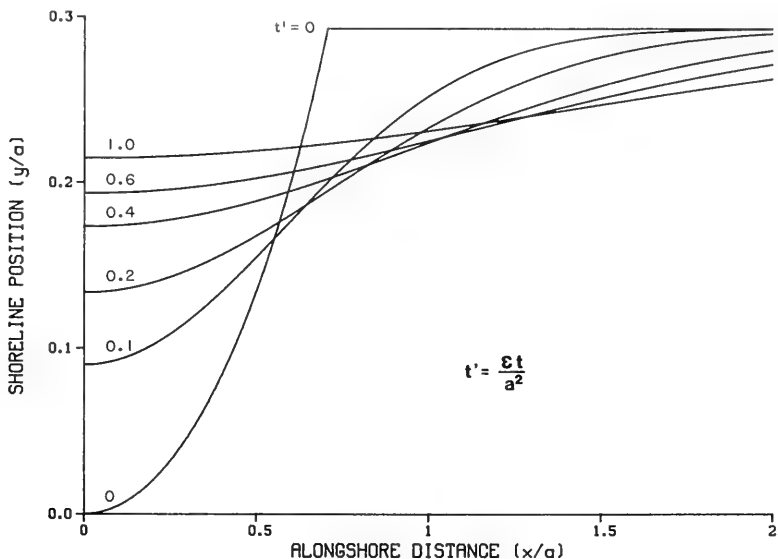


Figure 22. Shoreline evolution of an initially circular segment cut in a beach ( $\alpha = 45$  deg)

#### Rhythmic Beach

53. A beach with a rhythmic shoreline in the form of a cosine wave attenuates with time but maintains its rhythmic character. The initial condition is

$$y(x,0) = A \cos \sigma x \quad (43)$$

where  $A$  represents the amplitude of the rhythmic form such as cusps along the beach, and  $\sigma$  denotes the wave number of the shoreline oscillation or cusp. The quantity  $\sigma$  can be expressed also as  $2\pi/L$ , where  $L$  is the beach cusp wave length. The solution to this case is found to be



$$y(x,t) = A \cos \alpha x e^{-\sigma^2 \epsilon t} \quad (44)$$

for  $t > 0$  and  $-\infty < x < \infty$ .

Le Méhauté and Brebner (1961) and Bakker (1969) give this solution. A non-dimensional diagram of the shoreline evolution of an initially cosine-shaped beach is shown in Figure 23.

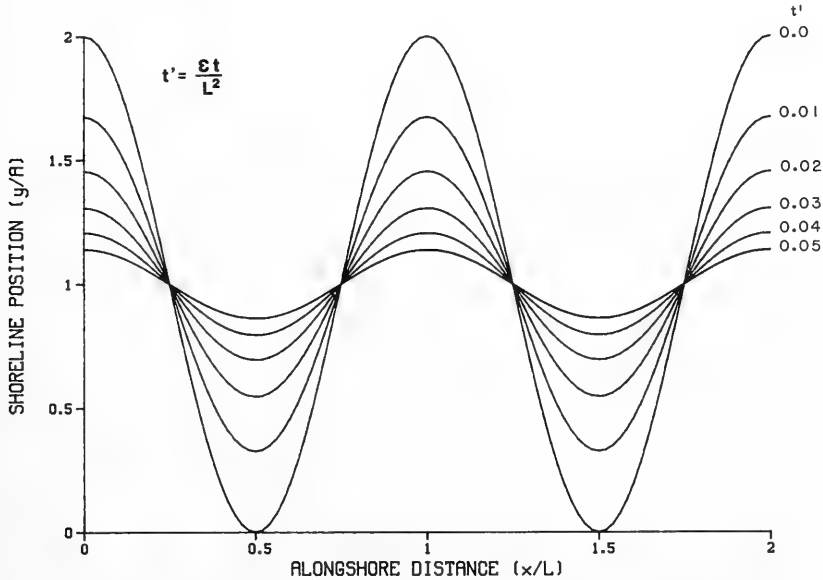


Figure 23. Shoreline evolution of an initially cosine-shaped beach (a distance of one beach cusp height added to the shoreline position)

#### Sand Discharge from a River Acting as a Point Source

54. If a river mouth is small in comparison to the area into which it is discharging sand, the discharge may be approximated by a point source. The sand discharge from the river or the strength of the point source is denoted as  $q_R$  and is a function of time. (The units of  $q_R$  are  $m^3/sec.$ ) A solution may be obtained by considering the continuous sand discharge from the river to be the sum of discretely released quantities of sand at consecutive

times. If a certain volume of sand  $V$  is instantaneously released at a point  $x_s$  at time  $t_s$ , the solution can be written

$$y(x,t) = \frac{V}{2D\sqrt{\pi\epsilon}(t-t_s)} e^{-\frac{(x-x_s)^2}{4\epsilon(t-t_s)}} \quad (45)$$

for  $t > t_s$  and  $-\infty < x < \infty$ .

Equation 45 has been discussed by Le Méhauté and Brebner (1961) and by Le Méhauté and Soldate (1977). Accordingly, a superposition of an infinite number of such released quantities can be used to represent the sand discharge from a river. According to Carslaw and Jaeger (1959, p. 262), the solution for a point source with a continuous time variable sand discharge  $q_R$  may be expressed as

$$y(x,t) = \frac{1}{2D\sqrt{\pi\epsilon}} \int_0^t q_R(\xi) e^{-\frac{(x-x_s)^2}{4\epsilon(t-\xi)}} \frac{d\xi}{\sqrt{t-\xi}} \quad (46)$$

for  $t > 0$  and  $-\infty < x < \infty$ .

If  $q_R$  is constant and equal to  $q_0$ , the solution is

$$y(x,t) = \frac{q_0}{D} \sqrt{\frac{t}{\pi\epsilon}} e^{-\frac{(x-x_s)^2}{4\epsilon t}} - \frac{q_0}{D} \frac{|x-x_s|}{2\epsilon} \operatorname{erfc} \frac{|x-x_s|}{2\sqrt{\epsilon t}} \quad (47)$$

for  $t > 0$  and  $-\infty < x < \infty$ .

Equation 47 is identical to the solution describing a constant flux  $q_0/2$  on the boundary ( $x = 0$ ) for a beach of semi-infinite extent. Figure 24 illustrates the solution where  $L$  is used as a normalizing length, and the point source is located at  $x_s = L$ . The nondimensional quantity containing the shoreline position is formed as the ratio between the amplitude of the sand transport rate and the sand discharge from the river.

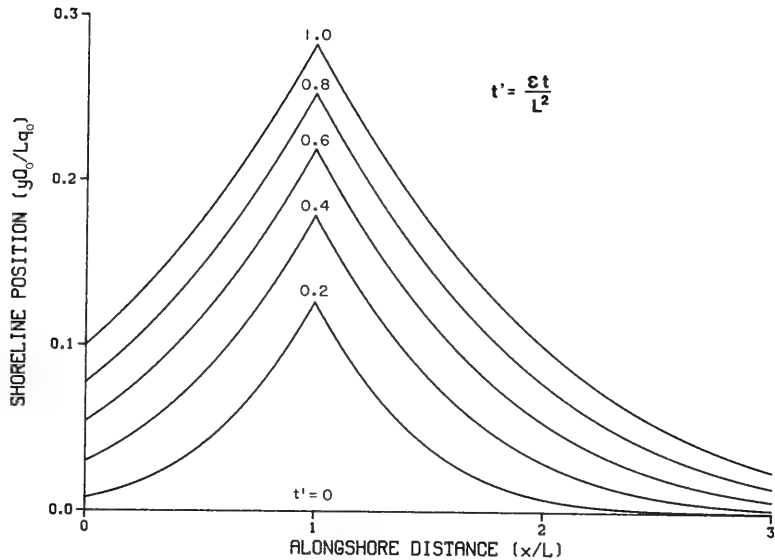


Figure 24. Shoreline evolution in the vicinity of a river discharging sand and acting as a point source

55. If the sand discharge has a periodic behavior, the function  $q_R$  could take the following form:

$$q_R(t) = q_0 + q_s \sin(\omega t + \phi) \quad (48)$$

where

$q_0$  = steady sand discharge from river

$q_s$  = amplitude of periodic sand discharge

$\omega$  = angular frequency =  $2\pi/T$

$T$  = period of oscillation of sand discharge from river

$\phi$  = phase angle of periodic variation

The solution consists of two parts, namely Equation 47 describing the shoreline evolution from a steady point source and the following solution which accounts for the periodic component:

$$y(x,t) = \frac{q_s}{D\sqrt{\epsilon}\pi} \int_0^{\sqrt{t}} \sin \left[ \omega(t - \xi^2) + \phi \right] e^{-x^2/4\epsilon\xi^2} d\xi \quad (49)$$

The shoreline behavior is composed of one contribution that evolves roughly proportional to the square root of elapsed time and another contribution which is a periodic oscillation that damps out along the x-axis with a decay factor  $\sqrt{\omega/2\epsilon}$  (both in the negative and positive directions). Consequently, beyond a certain distance from the discharge the periodic effect of Equation 49 can be neglected, implying that the solution may be approximated by Equation 47 only. Because of the periodic variation in the discharge, sand waves are generated from the river mouth. These sand waves propagate with a speed  $\sqrt{2\epsilon\omega}$  along the x-axis, and the time lag between the oscillation in sand discharge at the river mouth and a specific location is  $\pi/4 + x\sqrt{\omega/2\epsilon}$ . In Figure 25 the shoreline evolution at specific locations in the vicinity of a point source of sand discharge with a periodic variation in strength is shown as a function of

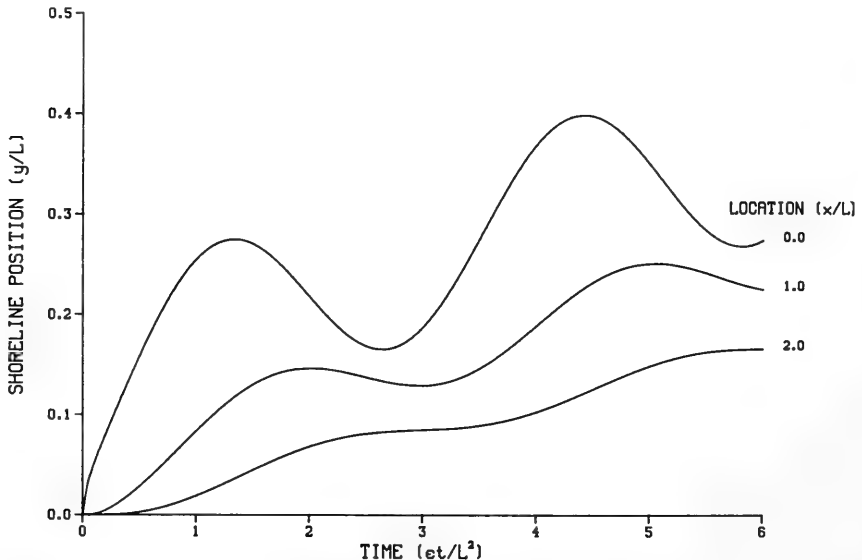


Figure 25. Shoreline evolution in the vicinity of a river discharging sand with a periodic variation in strength as a function of time

$$(\omega L^2/\epsilon = 2, \quad \phi = 0, \quad q_s/Q_o = q_o/Q_o = 0.5)$$

time. The quantities in the figure are dimensionless, with the sand discharge from the river normalized by the amplitude of the sand transport rate  $Q_0$  and the angular frequency of the oscillation normalized by  $\epsilon/L^2$ . Figure 25 clearly shows how the superimposed sinusoidal-shaped variation damps out with distance from the source along the x-axis.

### Sand Discharge from a River Mouth of Finite Length

56. If the river mouth has a finite width in comparison to the area into which it is discharging sand, an approximation by a point source is no longer accurate. Instead of supplying sand to the system via the boundary or initial conditions, the mass conservation equation in the full form of Equation 3 is applied. The sand discharge from the river  $q_R$  is considered a continuous function of  $x$ , varying along the river mouth. The river mouth is assigned a length  $2a$ , and the sand discharge is measured per unit width. Mathematically, the situation is expressed as

$$\epsilon \frac{\partial^2 y_1}{\partial x^2} + \frac{q_R}{D} = \frac{\partial y_1}{\partial t} \quad 0 \leq x \leq a \quad (50)$$

$$\epsilon \frac{\partial^2 y_2}{\partial x^2} = \frac{\partial y_2}{\partial t} \quad x > a \quad (51)$$

$$y_1(x, 0) = y_2(x, 0) = 0 \quad (52)$$

$$\frac{\partial y_1}{\partial x} = \frac{\partial y_2}{\partial x} \quad x = a$$

$$\frac{\partial y_1}{\partial x} = 0 \quad x = 0 \quad (53)$$

$$y_1 = y_2 \quad x = a$$

$$y_2 = 0 \quad x \rightarrow \infty \quad (54)$$

57. The problem consists of two coupled partial differential equations with appropriate boundary and initial conditions. Since the configuration is symmetric with respect to the center of the river mouth (if  $q_R$  is constant), only half of the problem domain has to be treated. The boundary conditions are no sand transport through the center of the river (symmetry), and mass conservation should apply between the two solution areas. Also, the beach must be continuous at all times over this boundary. Furthermore, the shoreline is unaffected by the river sand discharge as  $x$  approaches infinity. According to Carslaw and Jaeger (1959, p. 80) the solution is

$$y_1(x,t) = \frac{q_R t}{D} \left[ 1 - 2i^2 \operatorname{erfc} \left( \frac{a-x}{2\sqrt{\epsilon t}} \right) - 2i^2 \operatorname{erfc} \left( \frac{a+x}{2\sqrt{\epsilon t}} \right) \right] \quad (55)$$

for  $t > 0$  and  $0 \leq x \leq a$ .

$$y_2(x,t) = \frac{2q_R t}{D} \left[ i^2 \operatorname{erfc} \left( \frac{x-a}{2\sqrt{\epsilon t}} \right) - i^2 \operatorname{erfc} \left( \frac{x+a}{2\sqrt{\epsilon t}} \right) \right] \quad (56)$$

for  $t > 0$  and  $x > a$ .

58. The function  $i^2 \operatorname{erfc}$  is defined in Equation 23 and the superscript 2 denotes a double integration. An exponent  $n$  represents  $n$  integrations of the complementary error function. The following recurrence relation holds for  $n > 1$ :

$$2n i^n \operatorname{erfc} x = i^{n-2} \operatorname{erfc} x - 2x i^{n-1} \operatorname{erfc} x \quad (57)$$

In Figure 26 the solution to Equations 55 and 56 is illustrated.

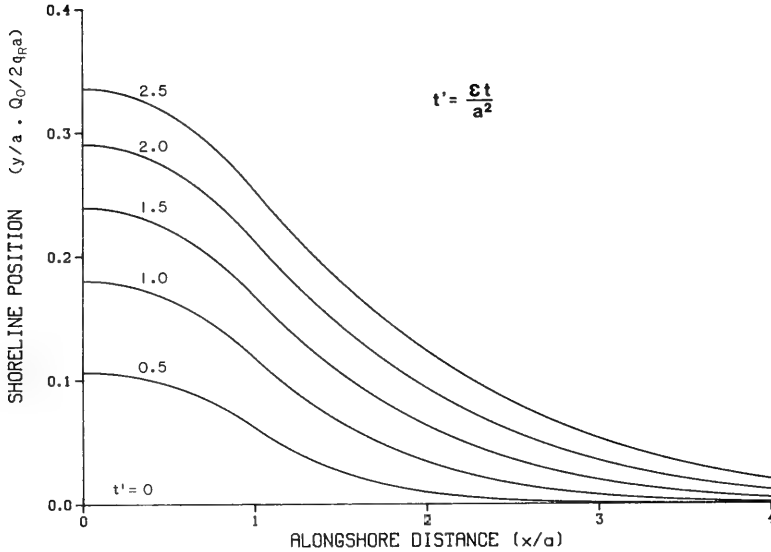


Figure 26. Shoreline evolution in the vicinity of a sand-discharging river mouth of finite width

59. A nondimensional quantity describing shoreline change is defined according to

$$y'(x', t') = \frac{y(x, t) \epsilon D}{4q_R a^2} \quad (58)$$

The quantity used to normalize Equation 58 can be written by using Equation 10 to arrive at

$$a \frac{2aq_R}{Q_0} \quad (59)$$

This quantity can be interpreted as a ratio between sand discharge from the river and the amplitude of the sand transport rate produced by the waves. The solutions given by Equations 47, 49, 55, and 56 are also valid for the placement of sand (beach nourishment), provided the placement is made under the same conditions. Solutions with an opposite sign consequently represent

mining of sand. Equations 55 and 56 describe only the general features of delta growth since the river flow conditions within the delta formation are neglected in the present treatment. The time required for the delta to reach a certain distance  $y_0$  from the original shoreline position is calculated from the following relationship

$$y_0(t) = \frac{q_R t}{D} \left[ 1 - 4i^2 \operatorname{erfc} \left( \frac{a}{2\sqrt{\epsilon t}} \right) \right] \quad (60)$$

for  $t > 0$  and  $x = 0$ .

Equation 60 is illustrated in the nondimensional diagram of Figure 27. For a specific wave climate, the above relation implies that an increase in the sand

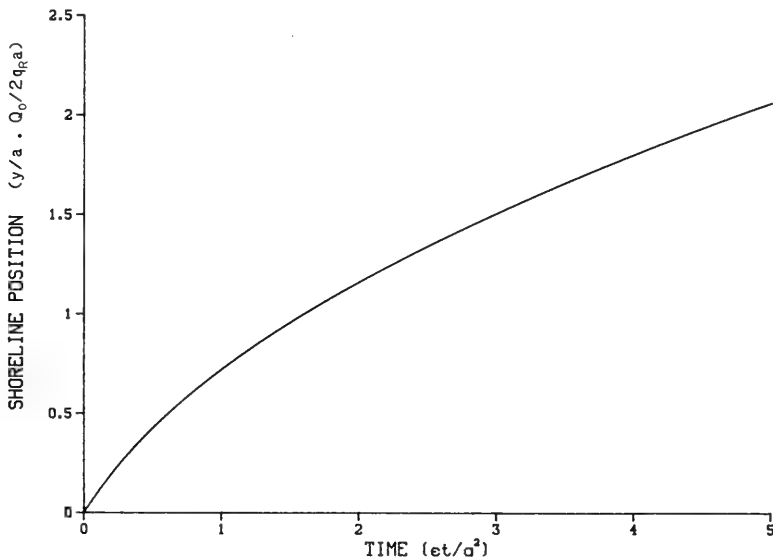


Figure 27. Maximum delta growth from a sand-discharging river mouth of finite length

discharge from the river has a proportional effect on the growth of the delta according to the following relation:



$$\frac{y_1}{y_2} = \frac{q_1}{q_2} \quad (61)$$

Here the indices 1 and 2 refer to two different sand discharge conditions experiencing the same wave climate.

PART III: SOLUTIONS FOR SHORELINE EVOLUTION  
INVOLVING COASTAL STRUCTURES

60. In the previous chapter, the incident wave crests were restricted to be parallel to the x-axis. In such a case, an initially straight beach will always remain straight, unless material is supplied in an irregular way. If the waves arrive at the same angle to the shoreline everywhere, the beach will also be stable if it is initially straight. However, if an obstacle on the beach disturbs the equilibrium transport conditions, a change in shoreline position occurs in order to achieve a new steady-state configuration. Examples of such obstacles are groins, jetties, detached breakwaters, and seawalls. In order to treat such complex cases analytically, the situation has to be idealized to a large degree. Properties which generally vary continuously along the shoreline (breaking wave angle, amplitude of the sand transport rate, etc.) usually must be approximated by means of a series of coupled solutions of simpler problems. Within each solution area the properties are held constant but are allowed to vary from one area to another.

Shoreline Change at Groins and Jetties

61. The analytical solution for beach change at a groin or any thin shore-normal structure which blocks alongshore sand transport was first obtained by Pelnard-Considère (1956). Initially, the beach is in equilibrium (parallel to the x-axis) with the same breaking wave angle existing everywhere, thus leading to a uniform sand transport rate along the beach. At time  $t = 0$  a thin groin is instantaneously placed at  $x = 0$ , blocking all transport. Mathematically, this boundary condition can be formulated as (see Equation 7)

$$\frac{\partial y}{\partial x} = \tan \alpha_0 \quad x = 0 \quad (62)$$

This equation states that the shoreline at the groin is at every instant parallel to the wave crests. The wave crests make an angle  $\alpha_0$  with the x-axis according to Figure 28, giving rise to longshore sand transport in the negative x-direction.

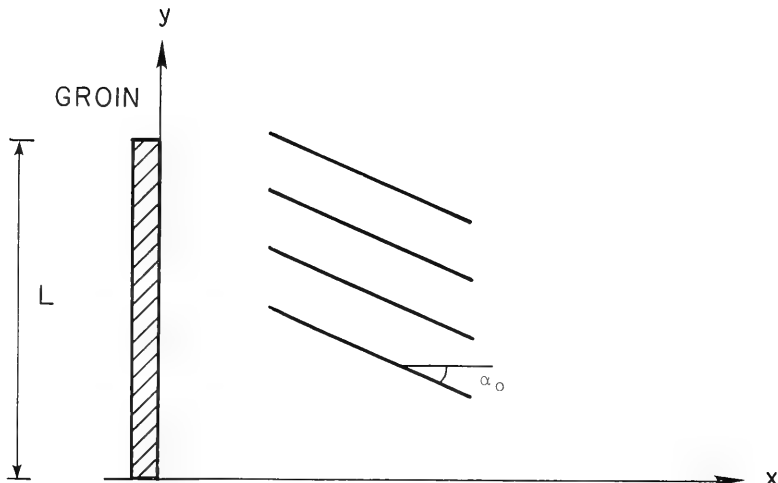


Figure 28. Definition sketch for the case of a groin

62. A groin interrupts the transport of sand alongshore, causing an accumulation at the updrift side and erosion at the downdrift side. The solution describing the accumulation part is

$$y(x,t) = 2 \tan \alpha_0 \sqrt{\epsilon t} \operatorname{ierfc} \left( \frac{x}{2\sqrt{\epsilon t}} \right) \quad (63)$$

for  $t > 0$  and  $x \geq 0$ .

The solution can also be written as follows:

$$y(x,t) = 2 \tan \alpha_0 \left[ \sqrt{\frac{\epsilon t}{\pi}} e^{-x^2/4\epsilon t} - \frac{x}{2} \operatorname{erfc} \left( \frac{x}{2\sqrt{\epsilon t}} \right) \right] \quad (64)$$

This expression is obtained by integrating the function  $\operatorname{ierfc}$  by parts. A nondimensional plot of the shoreline evolution updrift of a groin is shown in Figure 29.

63. The shoreline position has been normalized with a characteristic length (the groin length) and the tangent of the incident breaking wave angle.

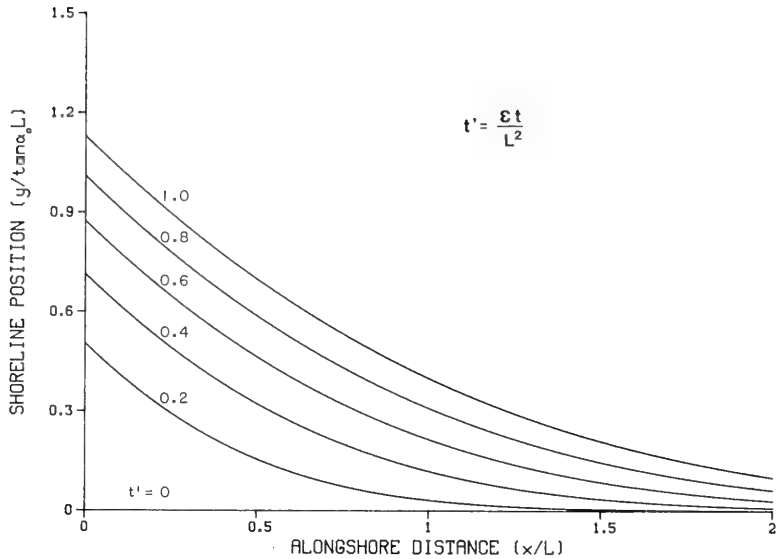


Figure 29. Shoreline evolution updrift of a groin which is totally blocking the transport of sand alongshore

For a specified amplitude of the sand transport rate and the depth of closure, the ratio of shoreline positions at a given point for two different incident breaking wave angles is proportional to the following ratio of respective tangents of the angles:

$$\frac{y_1}{y_2} = \frac{\tan \alpha_{o1}}{\tan \alpha_{o2}} \quad (65)$$

64. Equation 64 is valid only until the shoreline has reached the tip of the groin, after which time bypassing of sand is assumed to take place. This bypassing happens when  $y = L$  (length of the groin) at  $x = 0$ , which occurs at time  $t_G$ :

$$t_G = \frac{\pi}{\epsilon} \frac{L^2}{4 \tan^2 \alpha_o} \quad (66)$$

The above relationship for a fixed wave climate reveals that if the groin length is doubled, the time required for the shoreline to reach the end of the groin will increase fourfold.

65. If bypassing of a groin occurs, the boundary condition at  $x = 0$  changes into  $y = L$ . A correct solution to this situation should fulfill this boundary condition and use as an initial condition the shoreline shape just before bypassing occurred, according to Equation 64. An approximate solution was presented by Pelnard-Considère (1956) who used the solution for a shoreline with fixed position  $y_0$  at  $x = 0$  (see Equation 26) and matched it against Equation 64 by equating sand volumes. With this criterion, the following relationship between the time elapsed before bypassing occurs  $t_G$  (in Equation 64) and the actual time in the matching solution  $t_V$ , which makes the sand volumes equal, is obtained:

$$\frac{t_V}{t_G} = \frac{\pi^2}{16} \quad (67)$$

66. Thus, in the case of bypassing, it is possible to use Equation 26, if the time  $t$  is replaced by  $t_* = t - (1 - \pi^2/16)t_G$  for  $t > t_G$ . The rate of sand bypassing the groin for  $t > t_G$  is calculated according to Equation 8 to produce the following relationship:

$$Q = 2Q_0 \alpha_0 \left( 1 - \frac{L}{\alpha_0 \sqrt{\pi \epsilon t_*}} \right) \quad (68)$$

for  $t > t_G$ .

Here  $2Q_0 \alpha_0$  is the sand transport rate at equilibrium (straight beach) under imposed incident breaking wave angle  $\alpha_0$ , and  $t_*$  is the modified time in the matching solution using Equation 26.

67. Formally, the solution downdrift of a groin is the same as that in Equation 64 but with opposite sign. However, if the groin or jetty extends far outside the wave breaker line, diffraction will occur behind the groin altering the breaking wave height and angle; thus the transport capacity

(Equation 9) does not provide a complete description of the shoreline evolution if diffraction is significant.

68. Bypassing may occur immediately after construction of a groin and not start just at the time when the groin is completely filled. If the bypassing sand transport rate grows exponentially to a limiting value  $Q_B$  the boundary condition at the groin will be

$$\frac{\partial y}{\partial x} = \alpha_o - \frac{1}{2} \frac{Q_B}{Q_o} (1 - e^{-\gamma t}) \quad x = 0 \quad (69)$$

69. In Appendix B a derivation is given. The quantity  $\gamma$  is a rate coefficient describing the speed at which the bypassing sand discharge grows toward the limiting value  $Q_B$ . The solution downdrift of a groin may be written (for an initially straight beach) as

$$y(x,t) = -2 \left( \alpha_o - \frac{1}{2} \frac{Q_B}{Q_o} \right) \left[ \sqrt{\frac{\epsilon t}{\pi}} e^{-x^2/4\epsilon t} - \frac{x}{2} \operatorname{erfc} \left( \frac{x}{2\sqrt{\epsilon t}} \right) \right] - \frac{Q_B}{Q_o} \sqrt{\frac{\epsilon}{\pi}} e^{-\gamma t} \int_0^{\sqrt{t}} e^{\gamma \xi^2 - x^2/4\epsilon \xi^2} d\xi \quad (70)$$

for  $t > 0$  and  $x \geq 0$ .

Employing the two dimensionless parameters,  $Q_B/Q_o$  and  $\gamma L^2/\epsilon$ , the solution is illustrated in Figure 30.

70. The parameter  $\gamma L^2/\epsilon$  describes the rate at which the sand bypassing increases in comparison to the size of the coastal constant ( $\epsilon$ ). In Equation 70 the second term is a transient which decays with elapsed time. Accordingly, after sufficient elapsed time, Equation 70 will be identical to the solution given by Equation 64 with a modified incident breaking wave angle at  $x = 0$  ( $\tan \alpha_o \approx \alpha_o$ ). Equation 70 may be used also to describe shoreline change updrift of a groin (with reversed sign) if bypassing occurs immediately after construction of the groin. If, in Equation 70,  $Q_B/Q_o = 2\alpha_o$ , the

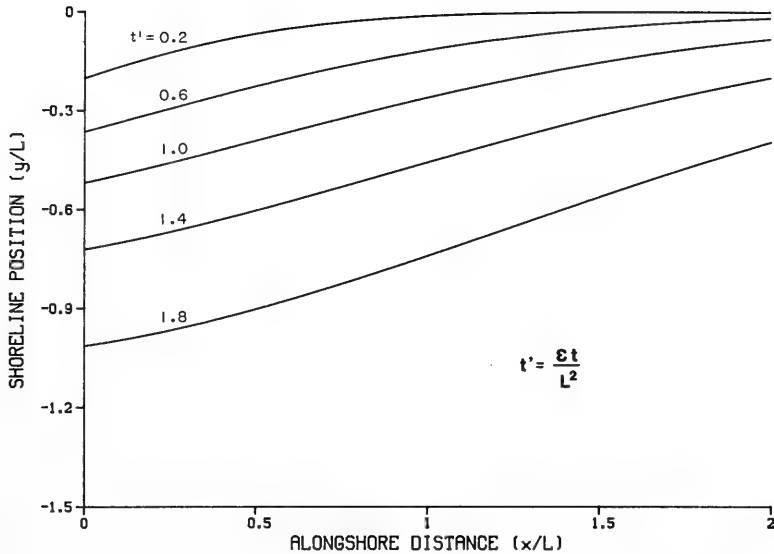


Figure 30. Shoreline evolution downdrift of a groin with bypassing described by  $Q_B(1 - e^{-\gamma t})$  ( $Q_B/Q_0 = 0.7$ ,  $\alpha_0 = 0.4$  rad,  $\gamma L^2/\epsilon = 2$ )

bypassing sand discharge will equal the transport rate alongshore behind the groin at equilibrium conditions. Consequently, the initially eroded area downdrift of the groin will fill when the bypassing sand rate reaches its maximum, and the beach will become straight again.

71. In order to investigate the effects of the linearization of the governing equation (Equation 9) on the solution for a groin, numerical simulations were carried out with the original sand transport equation (Equation 7). Selected results are displayed in Figures 31 and 32. From the two figures it is seen that the linearization procedure degrades the solution if the incident breaking wave angle is about 30 deg. However, the analytical solution has surprising accuracy, considering the approximations made.

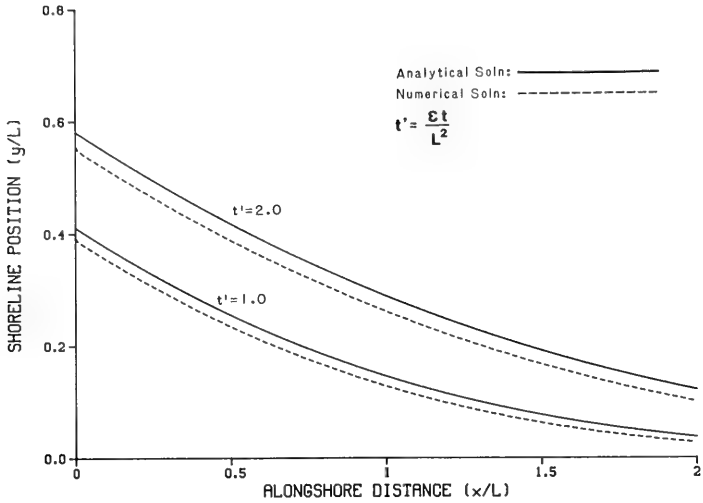


Figure 31. Comparison between analytical and numerical solutions of shoreline evolution updrift of a groin with incident breaking wave angle 20 deg

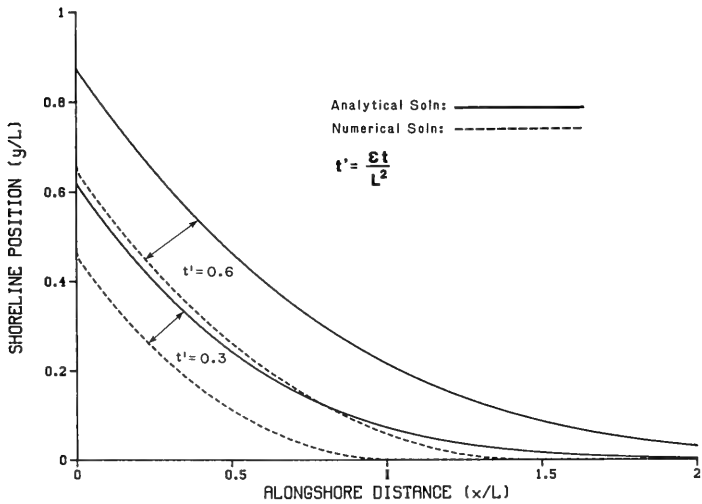


Figure 32. Comparison between analytical and numerical solutions of shoreline evolution updrift of a groin with incident breaking wave angle 45 deg



Initially Filled Groin System

72. Dean (1984) presents an analytical solution for shoreline evolution between two identical groins which define a compartment initially filled with sand. The distance between the groins is denoted by  $W$ , and the groin length is  $L$ . At time  $t = 0$ , the shoreline is exposed to the action of waves breaking with angle  $\alpha_o$ . The solution is

$$y(x,t) = L - W\left(1 - \frac{x}{W}\right) \tan \alpha_o + \frac{2 \tan \alpha_o}{W} \sum_{n=0}^{\infty} \left\{ \left[ \frac{2W}{(2n+1)\pi} \right]^2 e^{-\epsilon(2n+1)^2 \pi^2 t / 4W^2} \cos \left[ \frac{(2n+1)\pi x}{2W} \right] \right\} \quad (71)$$

for  $t > 0$  and  $0 \leq x \leq W$ .

The boundary conditions for this configuration are no sand transport at  $x = 0$  ( $\partial y / \partial x = \tan \alpha_o$ ) and a constant shoreline position of  $y = L$  at  $x = W$ . Consequently, bypassing occurs at the boundary  $x = W$ , whereas no sand enters the system at  $x = 0$ . This occurrence means that the solution is unsuitable for application to a groin system of more than one compartment. Otherwise, bypassing must be accounted for in the boundary conditions at the updrift groin (left) in each compartment leading to a coupled problem. The last term in Equation 71 approaches zero as  $t \rightarrow \infty$  and causes a shoreline parallel to the wave crests to be created between the groins. In Figure 33 the analytical solution is presented in dimensionless form. All distances have been normalized with the compartment width  $W$ .

73. The final percentage loss of sand from the groin compartment is

$$\frac{1}{2} \frac{W}{L} \tan \alpha_o \quad (72)$$

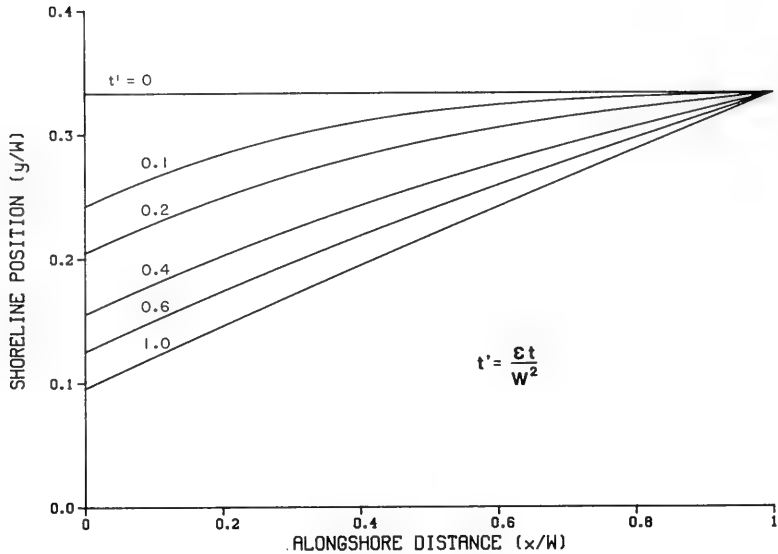


Figure 33. Shoreline evolution between two groins initially filled with sand ( $L/W = 0.33$  ,  $\alpha_0 = 0.25$  rad)

From Equation 71, the sand bypassed (discharge rate) at  $x = W$  can be obtained. The sand transport rate as a function of time can be written (if it is assumed that  $\tan \alpha_0 \approx \alpha_0$ )

$$Q(t) = 4Q_0\alpha_0 \sum_{n=0}^{\infty} (-1)^n \frac{2}{(2n+1)\pi} e^{-\epsilon(2n+1)^2\pi^2 t/4W^2} \quad (73)$$

for  $t > 0$  and  $x = W$ .

In Equation 73, the quantity  $2Q_0\alpha_0$  is the sand transport rate along a straight beach exposed to the incident breaking wave angle  $\alpha_0$ . (This is the transport initially existing when the groin compartment is completely filled.) If  $Q$  in Equation 73 is normalized with this quantity, the bypassing sand discharge at the downdrift end groin is conveniently displayed in dimensionless form. Figure 34 shows such a curve.

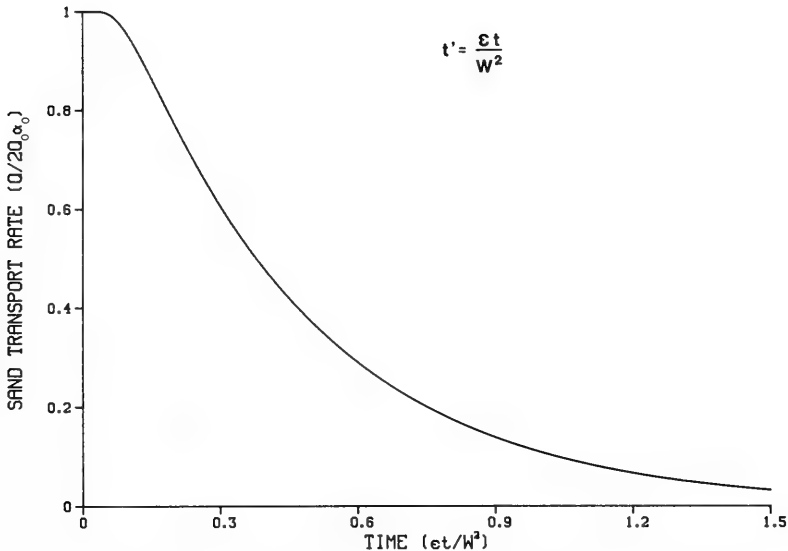


Figure 34. Bypassing sand transport rate at the downdrift end of a groin  $x = W$  as a function of time

#### Shoreline Change at a Detached Breakwater

74. A detached breakwater reduces the wave height behind it and produces a circular wave pattern at each tip, thus decreasing the longshore sand transport rate. The actual effects are quite complex to describe and involve diffraction and the current field resulting from spatial changes in wave height and direction. However, it is possible to find an analytical solution if the situation is idealized.

75. It is assumed that the incident breaking wave crests are parallel to the  $x$ -axis and to the detached breakwater. When the waves reach the breakwater, they are assumed to be diffracted at a constant angle behind the breakwater (shadowed region) and remain parallel to the  $x$ -axis outside of the breakwater (the illuminated region). The diffraction behind the breakwater is symmetric about the center of the breakwater and, accordingly, only half of the problem domain needs to be considered. In Figure 35, a definition sketch is shown.

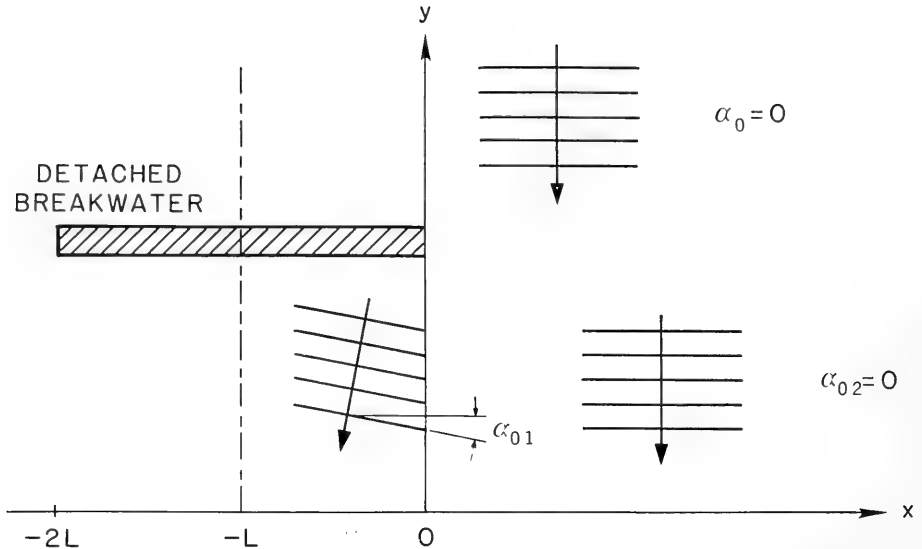


Figure 35. Definition sketch for the problem of shoreline change in the vicinity of a detached breakwater

76. Since the incident breaking wave angles and the amplitudes of the sand transport rates  $Q_{o1}$  and  $Q_{o2}$ , respectively, are different in the shadowed and illuminated regions, a coupled problem arises. The boundary conditions for this case are as follows:

- a. No sand should be transported across the line of symmetry behind the breakwater.
- b. The sand transport rate out of the area on the right side of the breakwater should be equal to that into the area behind the breakwater.
- c. The shoreline is continuous over the boundary between the two areas.

Furthermore, the shoreline should be undisturbed ( $y = 0$ ) far from the structure. With  $y_1$  denoting the shoreline position in solution area number 1 (shadow region) and  $y_2$  denoting the shoreline position in solution area number 2 (the illuminated region), the mathematical formulation of the situation is

$$\epsilon_1 \frac{\partial^2 y_1}{\partial x^2} = \frac{\partial y_1}{\partial t} \quad -L \leq x \leq 0 \quad (74)$$

$$\epsilon_2 \frac{\partial^2 y_2}{\partial x^2} = \frac{\partial y_2}{\partial t} \quad x > 0 \quad (75)$$

$$y_1(x, 0) = y_2(x, 0) = 0 \quad (76)$$

$$\frac{\partial y_1}{\partial x} = \tan \alpha_{o1} \quad x = -L \quad (77)$$

$$\frac{\partial y_1}{\partial x} = \frac{\partial y_2}{\partial x} \frac{Q_{o2}}{Q_{o1}} + \alpha_{o1} \quad x = 0 \quad (78)$$

$$y_1 = y_2 \quad x = 0$$

$$y_2 = 0 \quad x \rightarrow \infty \quad (79)$$

77. The derivation of this solution is presented in Appendix C. The quantities  $Q_{o1}$  and  $Q_{o2}$  are the amplitudes of the longshore sand transport rate in the respective areas, and  $\alpha_{o1}$  is the diffracted breaking wave angle behind the breakwater. The angle  $\alpha_{o2}$  is zero since the wave crests in this area are parallel to the x-axis throughout time. The solution is, with

$$\delta = \sqrt{\frac{\epsilon_1}{\epsilon_2}} = \sqrt{\frac{Q_{o1}}{Q_{o2}}} \quad (80)$$

$$\begin{aligned}
y_1(x,t) = & -\frac{\delta\alpha_{o1}}{\delta+1} 2\sqrt{\epsilon_1 t} \operatorname{ierfc}\left(\frac{-x}{2\sqrt{\epsilon_1 t}}\right) \\
& + \tan\alpha_{o1} \sum_{n=0}^{\infty} \left\{ \left(\frac{\delta-1}{\delta+1}\right)^n 2\sqrt{\epsilon_1 t} \operatorname{ierfc}\left[\frac{(2n+1)L+x}{2\sqrt{\epsilon_1 t}}\right] \right. \\
& \left. + \left(\frac{\delta-1}{\delta+1}\right)^{n+1} 2\sqrt{\epsilon_1 t} \operatorname{ierfc}\left[\frac{(2n+1)L-x}{2\sqrt{\epsilon_1 t}}\right] \right\} \\
& - \frac{\delta\alpha_{o1}}{\delta+1} \sum_{n=0}^{\infty} \left\{ \left(\frac{\delta-1}{\delta+1}\right)^n 2\sqrt{\epsilon_1 t} \operatorname{ierfc}\left[\frac{2(n+1)L+x}{2\sqrt{\epsilon_1 t}}\right] \right. \\
& \left. + \left(\frac{\delta-1}{\delta+1}\right)^{n+1} 2\sqrt{\epsilon_1 t} \operatorname{ierfc}\left[\frac{2(n+1)L-x}{2\sqrt{\epsilon_1 t}}\right] \right\} \quad (81)
\end{aligned}$$

for  $t > 0$  and  $-L \leq x \leq 0$ .

$$\begin{aligned}
y_2(x,t) = & -\frac{\delta\alpha_{o1}}{\delta+1} 2\sqrt{\epsilon_1 t} \operatorname{ierfc}\left(\frac{\delta x}{2\sqrt{\epsilon_1 t}}\right) \\
& - 2 \frac{\delta^2\alpha_{o1}}{(\delta+1)^2} \sum_{n=0}^{\infty} \left\{ \left(\frac{\delta-1}{\delta+1}\right)^n 2\sqrt{\epsilon_1 t} \operatorname{ierfc}\left[\frac{\delta x + 2(n+1)L}{2\sqrt{\epsilon_1 t}}\right] \right\} \\
& + 2 \frac{\delta \tan\alpha_{o1}}{\delta+1} \sum_{n=0}^{\infty} \left\{ \left(\frac{\delta-1}{\delta+1}\right)^n 2\sqrt{\epsilon_1 t} \operatorname{ierfc}\left[\frac{\delta x + (2n+1)L}{2\sqrt{\epsilon_1 t}}\right] \right\} \quad (82)
\end{aligned}$$

for  $t > 0$  and  $x > 0$ .

78. The distance  $L$  is half the length of the detached breakwater. If Equations 81 and 82 are plotted, the following behavior will be noticed. When the breakwater is placed in front of the initially straight shoreline at time  $t = 0$ , erosion of the shoreline starts at points in line with the corners of the breakwater. Simultaneously, the shoreline grows to form a salient about the line of symmetry behind the breakwater. Because of the gradient of the shoreline outside the shadow of the breakwater, material is transported toward the breakwater in order to achieve a state of equilibrium with the waves. The shoreline behind the breakwater also approaches an equilibrium configuration which is parallel to the wave crests diffracted at the angle  $\alpha_{01}$ . The final shoreline will be inclined at an angle  $\alpha_{01}$  behind the breakwater and be straight outside the breakwater. However, the straight portion of the shoreline will at all times be displaced landward a small distance, controlled by the volume of sand that has accumulated behind the breakwater. Figure 36 illustrates the solution in dimensionless form for

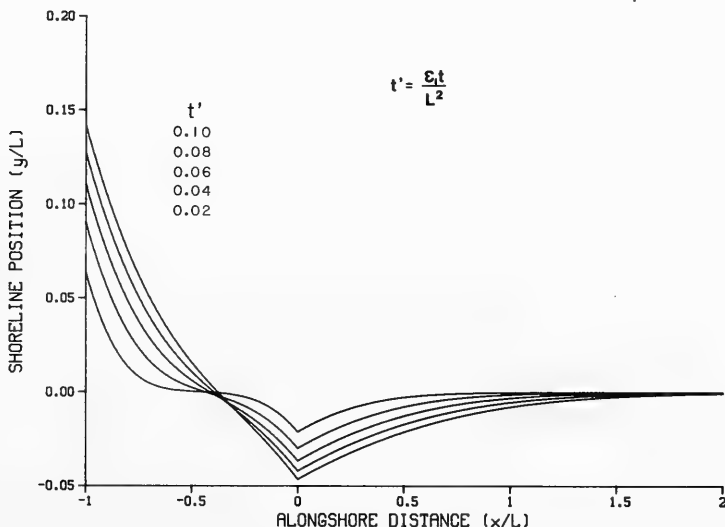


Figure 36. Initial shoreline evolution in the vicinity of a shore-parallel detached breakwater ( $\delta = 0.5$ ,  $\alpha_{01} = 0.4$  rad,  $\alpha_{02} = 0$ )

short elapsed times, and Figure 37 shows the features of the solution after a long elapsed time. The length of the salient behind the breakwater increases in time toward a maximum value of

The elapsed time is normalized by the quantity  $L^2/\epsilon_1$ . Although mass is conserved across the boundary between the two solution areas, the gradient of the shoreline is not continuous at this point.

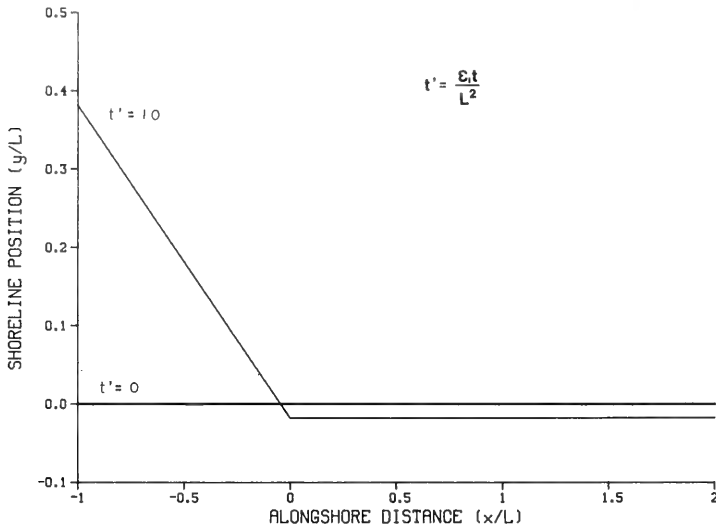


Figure 37. Final shoreline position in the vicinity of a shore-parallel detached breakwater ( $\delta = 0.5$ ,  $\alpha_{01} = 0.4$  rad,  $\alpha_{02} = 0$ )

#### Shoreline Change at a Seawall

79. The function of a seawall is to prevent the shoreline from retreating along a specific coastal reach. If the shoreline remains well seaward of the seawall, there will be no influence of the seawall on the shoreline evolution. If the shoreline retreats to the seawall, the location of the seawall determines the minimum allowable shoreline position. If erosion takes place beside a seawall (flanking), various changes in the shoreline position might occur depending on the characteristics of the seawall and the incident waves. If flanking of the seawall is not possible (see Figure 38), the solution for the plan shape of an eroded shoreline will be the same as for erosion downdrift of a groin (Equation 64, with opposite sign). In this case, the seawall is functioning as a semi-infinite structure.



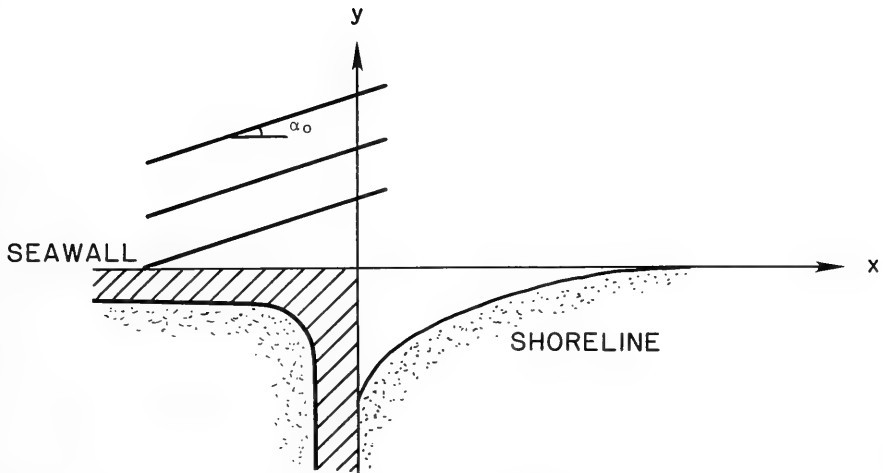


Figure 38. Definition sketch for a semi-infinite seawall for which no erosion occurs behind the seawall

80. Figure 39 illustrates the case of erosion at the side and behind a seawall, i.e., flanking of the seawall. This must be solved as a coupled problem. The incident breaking wave angle is  $\alpha_{02}$  outside the seawall and  $\alpha_{01}$  behind it. Wave energy is transported behind the seawall by the process of diffraction.

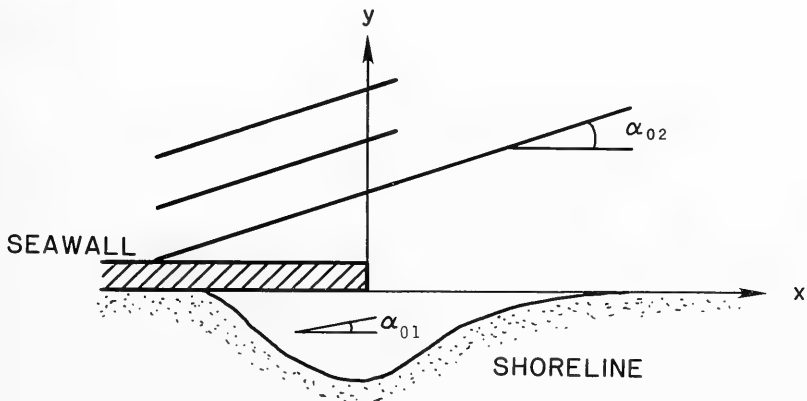


Figure 39. Definition sketch for a semi-infinite seawall for which erosion occurs behind the seawall

81. The ratio between the amplitudes of the longshore sand transport rate in the two solution areas will be denoted as  $\delta^2 (= Q_{o1}/Q_{o2})$ . Mathematically, the situation is formulated as

$$\epsilon_1 \frac{\partial^2 y_1}{\partial x^2} = \frac{\partial y_1}{\partial t} \quad x \leq 0 \quad (84)$$

$$\epsilon_2 \frac{\partial^2 y_2}{\partial x^2} = \frac{\partial y_2}{\partial t} \quad x > 0 \quad (85)$$

$$y_1(x,0) = y_2(x,0) = 0 \quad (86)$$

$$\frac{\partial y_1}{\partial x} = \alpha_{o1} - \frac{1}{\delta^2} \alpha_{o2} + \frac{1}{\delta^2} \frac{\partial y_2}{\partial x} \quad x = 0 \quad (87)$$

$$y_1 = y_2 \quad x = 0 \quad (88)$$

$$y_1 = 0 \quad x \rightarrow \infty$$

$$y_2 = 0 \quad x \rightarrow \infty \quad (89)$$

It is assumed that the border between the two solution areas at  $x = 0$  is stationary in time, although it moves somewhat in the  $x$ -direction as time evolves. The solution is (for details, see Appendix D)

$$y_1(x,t) = \frac{\alpha_{o1} - \frac{1}{\delta^2} \alpha_{o2}}{1 + \frac{1}{\delta}} \left[ 2 \sqrt{\frac{\epsilon_1 t}{\pi}} e^{-x^2/4\epsilon_1 t} + x \operatorname{erfc} \left( \frac{-x}{2\sqrt{\epsilon_1 t}} \right) \right] \quad (90)$$

for  $t > 0$  and  $x \leq 0$ .

$$y_2(x,t) = \frac{\alpha_{o1} - \frac{1}{\delta^2} \alpha_{o2}}{1 + \frac{1}{\delta}} \left[ 2 \sqrt{\frac{\varepsilon_1 t}{\pi}} e^{-\delta^2 x^2 / 4 \varepsilon_1 t} - \delta x \operatorname{erfc} \left( \frac{\delta x}{2 \sqrt{\varepsilon_1 t}} \right) \right] \quad (91)$$

for  $t > 0$  and  $x > 0$ .

The quantity  $\alpha_{o1}$  represents a mean diffracted wave angle behind the seawall. The solution in nondimensional form is presented in Figure 40 (expressed in terms of the coastal constant  $\varepsilon_1$ ).

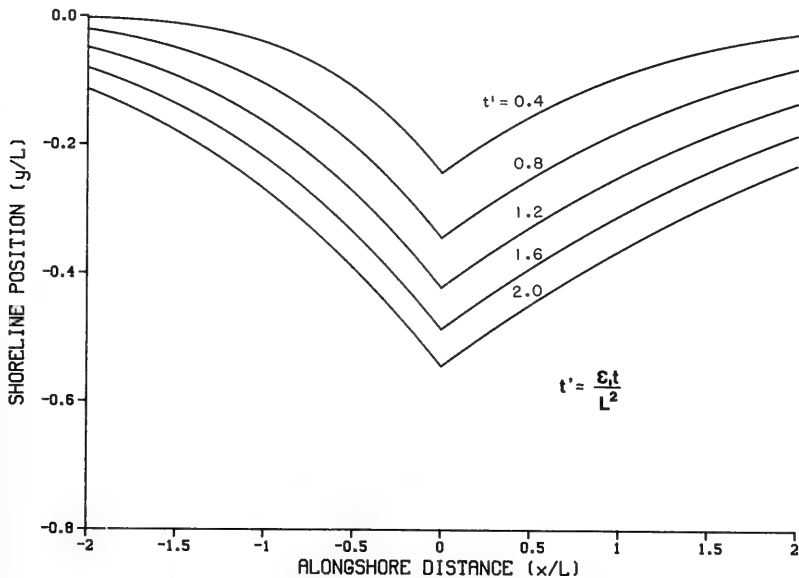


Figure 40. Shoreline evolution in the vicinity of a seawall where erosion and flanking may occur behind it ( $\alpha_{o1} = 0.2$  rad,  $\alpha_{o2} = 0.4$  rad,  $\delta = 0.6$ )

82. A characteristic length  $L$  is chosen to normalize the shoreline position. In Figure 40 the time has been normalized by use of the quantity  $L^2/\varepsilon_1$ .

#### Shoreline Change at a Jetty, Including Diffraction

83. In the shadow zone of a long groin or jetty, it may be an

oversimplification to neglect the process of wave diffraction. Consequently, although Equation 64 (with reversed sign) may give a satisfactory description of shoreline evolution at some distance downdrift of a jetty, in the vicinity of the jetty this solution does not represent what is commonly observed. Erosion just behind the jetty will be overestimated if diffraction is neglected since the wave height is assumed to be constant alongshore. Accordingly, by allowing a variation in wave height (and thus in the amplitude of the sand transport rate) in the shadow zone, a more realistic description of shoreline change will be obtained.

84. There are a number of ways to account for a varying amplitude in the longshore sand transport rate (resulting from varying wave height). One way is to assume that, outside the shadow zone, the incident breaking wave angle and the amplitude of the sand transport rate are not influenced by the jetty. In the vicinity of the jetty, Equation 11 may be used to account for a variation in the amplitude of the sand transport rate. An alternative way is to divide the shadow region into distinct solution areas, each having a constant amplitude of the sand transport rate. The incident breaking wave angle may also be varied from one solution area to another. With this procedure, a coupled system of equations is obtained which involves intensive calculations for even a small number of solution areas. If the simple case of two solution areas (one inside the shadow zone and one outside) is considered, the mathematical formulation is the same as for a detached breakwater. However, the incident breaking wave angle outside the shadow region is not zero (in which case no sand transport would occur) but has a finite value. Therefore, the boundary condition on continuity in sand transport across the border between the two solution areas takes the following form:

$$\frac{\partial y_1}{\partial x} = \alpha_{o1} - \frac{1}{\delta^2} \alpha_{o2} + \frac{1}{\delta^2} \frac{\partial y_2}{\partial x} \quad (92)$$

where  $\delta^2$  is the ratio between the amplitudes of the sand transport rate inside and outside the shadow region. The analytical solution to this problem is formally identical to Equations 81 and 82, except that certain constants are different. The following substitutions should be made in order to apply Equation 81 and Equation 82 to the diffracting jetty case:

$$-\frac{\delta\alpha_{o1}}{\delta+1} \rightarrow \frac{-\delta^2\alpha_{o1} + \alpha_{o2}}{\delta(\delta+1)} \quad (93)$$

$$-\frac{\delta^2\alpha_{o1}}{(\delta+1)^2} \rightarrow \frac{-\delta^2\alpha_{o1} + \alpha_{o2}}{(\delta+1)^2} \quad (94)$$

85. If  $\alpha_{o2}$  is zero, the expressions on the right side reduce to those on the left side. As can be seen from Equations 81 and 82, even though the description involves only two solution areas, the governing equation is already quite complex. Generalization to an arbitrary number of solution areas is straightforward, in which case the situation is mathematically expressed for the  $i^{\text{th}}$  area as follows (see Figure 41):

$$\epsilon_i \frac{\partial^2 y_i}{\partial x^2} = \frac{\partial y_i}{\partial t} \quad x_i \leq x \leq x_{i+1} \quad (95)$$

$$\frac{\partial y_i}{\partial x} = \alpha_{oi} - \frac{1}{\delta_i^2} \alpha_{oi+1} + \frac{1}{\delta_i^2} \frac{\partial y_{i+1}}{\partial x} \quad x = x_{i+1} \quad (96)$$

$$\frac{\partial y_{i-1}}{\partial x} = \alpha_{oi-1} - \frac{1}{\delta_{i-1}^2} \alpha_{oi} + \frac{1}{\delta_{i-1}^2} \frac{\partial y_i}{\partial x} \quad x = x_i \quad (97)$$

$$y_{i-1} = y_i \quad x = x_i$$

$$y_i = y_{i+1} \quad x = x_{i+1} \quad (98)$$

where

$$\delta_i^2 = \frac{Q_{oi}}{Q_{oi+1}} \quad (99)$$

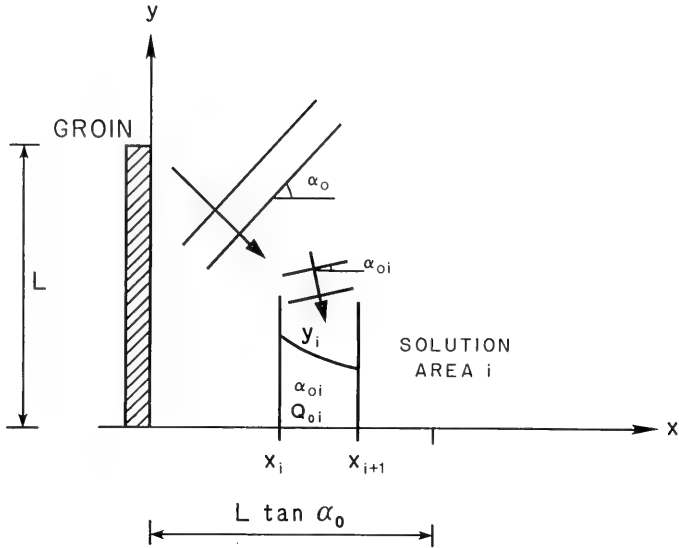


Figure 41. Definition sketch for shoreline evolution downdrift of a jetty for which a finite number of solution areas is used to model diffraction

For the first and last solution areas, other conditions prevail on the outer boundaries, such as no sand transport at the jetty, and  $y = 0$  as  $x \rightarrow +\infty$ .

86. Extremely complex algebraic manipulations are associated with the analytical solution of coupled systems with several solution areas. In Figure 42 the solution is presented for two areas, with  $\alpha_{o1} = -0.1$  rad,  $\alpha_{o2} = -0.4$  rad, and  $\delta = 0.5$ .

87. The solution for an arbitrary number of distinct areas is outlined in Appendix E. In Figure 42 are plotted shoreline positions normalized with the length of the shadow region. The length of the geometric shadow region is  $B = L \tan(\alpha_o)$ , where  $L$  is the jetty length and  $\alpha_o$  is the incident breaking wave angle in the illuminated region.

88. If the amplitude of the longshore sand transport rate is considered to be a continuous function of  $x$  in the shadow zone, Equation 11 is applicable. However, this equation is quite complex, and it is difficult to find analytical solutions even if very simple functions are employed. The related case, in which the incident breaking wave angle is a continuous function of

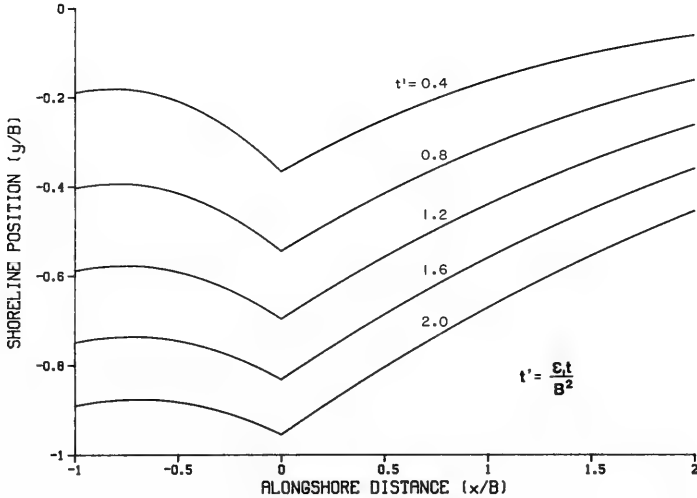


Figure 42. Shoreline evolution in the vicinity of a groin for variable sand transport rate conditions (two solution areas;  $\delta = 0.5$ ,  $\alpha_{01} = -0.1$  rad,  $\alpha_{02} = -0.4$  rad)

$x$ , is easier to treat analytically and provides interesting solutions. Under these circumstances, Equation 11 will take the following form:

$$\frac{\partial^2 y}{\partial x^2} = \frac{1}{\epsilon} \frac{\partial y}{\partial t} + \frac{d\alpha_0}{dx} \quad (100)$$

in which  $\alpha_0$  is a function of  $x$  only. This is formally the same equation as that describing heat conduction in a solid containing a finite source. Consequently, if  $\alpha_0$  grows linearly with  $x$  ( $\alpha_0 = x\alpha_m/B$ ) the situation will be identical to the one describing a river mouth of finite length which discharges sand at a constant rate. Equations 55 and 56 are the solutions to this case, with reversed sign and  $q_R$  replaced by  $\alpha_m/B$ . The solution is presented in Figure 26 in dimensionless form.

89. If  $\alpha_0$  is different from zero at the jetty, but still grows linearly along the  $x$ -axis in the shadow zone, the variation in breaking wave angle will be

$$\alpha_0 = \alpha_v + \left( \alpha_H - \alpha_v \right) \frac{x}{B} \quad (101)$$

in which  $\alpha_v$  is the incident breaking wave angle at the jetty, and  $\alpha_H$  is the angle in the illuminated region. The mathematical description for this case is almost the same as for a river mouth of finite length which discharges sand but with a modified source term. This is a coupled problem containing two solution areas but with a boundary condition at the jetty given by

$$\frac{\partial y_1}{\partial x} = \tan \alpha_v \quad (102)$$

The analytical solution to this problem is (see Appendix F)

$$y_1(x,t) = \frac{(\alpha_H - \alpha_v)\epsilon t}{B} \left[ 2i^2 \operatorname{erfc} \left( \frac{B-x}{2\sqrt{\epsilon t}} \right) + 2i^2 \operatorname{erfc} \left( \frac{B+x}{2\sqrt{\epsilon t}} \right) - 1 \right] \\ - \tan \alpha_v \left[ 2 \sqrt{\frac{\epsilon t}{\pi}} e^{-x^2/4\epsilon t} - x \operatorname{erfc} \left( \frac{x}{2\sqrt{\epsilon t}} \right) \right] \quad (103)$$

for  $t > 0$  and  $0 \leq x \leq B$ .

$$y_2(x,t) = \frac{(\alpha_H - \alpha_v)\epsilon t}{B} \left[ 2i^2 \operatorname{erfc} \left( \frac{x+B}{2\sqrt{\epsilon t}} \right) - 2i^2 \operatorname{erfc} \left( \frac{x-B}{2\sqrt{\epsilon t}} \right) \right] \\ - \tan \alpha_v \left[ 2 \sqrt{\frac{\epsilon t}{\pi}} e^{-x^2/4\epsilon t} - x \operatorname{erfc} \left( \frac{x}{2\sqrt{\epsilon t}} \right) \right] \quad (104)$$

for  $t > 0$  and  $x > B$ .

The quantity  $B$  is the geometric length of the shadow zone as before. In Figure 43, the dimensionless shoreline evolution is presented for the specific case of  $\alpha_v = -0.1$  rad and  $\alpha_H = 0.4$  rad. Shoreline position has been normalized by the length of the shadow region.

90. Another case that allows a fairly easy analytical solution is obtained by assuming that the incident breaking wave angle varies exponentially with distance from the jetty according to



$$\alpha_o = \alpha_m (1 - e^{-\gamma x}) \quad (105)$$

Here, the quantity  $\gamma$  is a coefficient describing the rate at which the breaking wave angle approaches the undisturbed value  $\alpha_m$  along the x-axis.

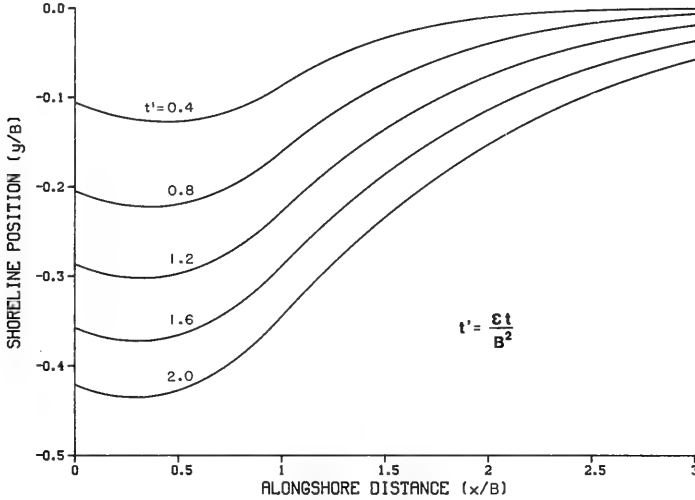


Figure 43. Shoreline evolution behind a jetty with linear variation in breaking wave angle in the shadow zone ( $\alpha_v = -0.1$  rad,  $\alpha_H = 0.4$  rad)

The derivation of the analytical solution is presented in Appendix G. The solution is

$$y(x,t) = \frac{\alpha_m \gamma}{2} \left[ -\frac{4}{\gamma} \sqrt{\frac{\epsilon t}{\pi}} e^{-x^2/4\epsilon t} + 2 \frac{x}{\gamma} \operatorname{erfc} \left( \frac{x}{2\sqrt{\epsilon t}} \right) + \frac{1}{\gamma^2} e^{-\gamma x + \epsilon t \gamma^2} \operatorname{erfc} \left( \frac{x}{2\sqrt{\epsilon t}} - \gamma\sqrt{\epsilon t} \right) - \frac{1}{\gamma^2} e^{\gamma x + \epsilon t \gamma^2} \operatorname{erfc} \left( \frac{x}{2\sqrt{\epsilon t}} + \gamma\sqrt{\epsilon t} \right) \right] + \frac{\alpha_m}{\gamma} e^{-\gamma x} (1 - e^{-\gamma^2 \epsilon t}) \quad (106)$$

for  $t > 0$  and  $x \geq 0$ .

If a dimensionless quantity  $\gamma L$  is introduced, the solution may be displayed efficiently in dimensionless form (Figure 44). For large values of  $\gamma$ , Equation 106 approaches Equation 64, which is valid for a jetty and constant oblique breaking wave angle.

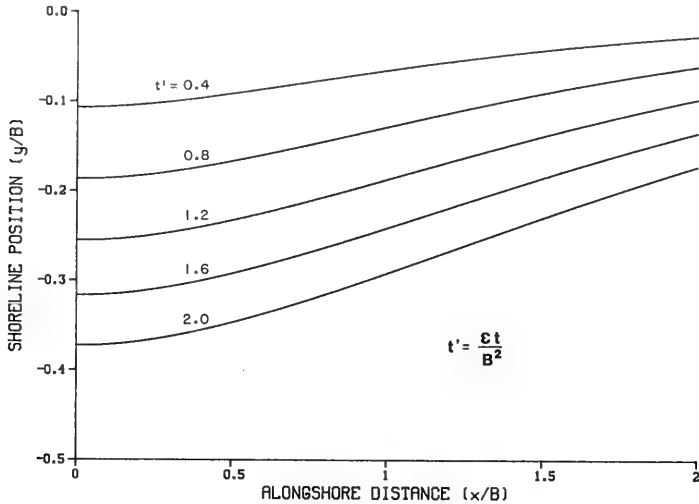


Figure 44. Shoreline evolution behind a jetty with exponential variation in breaking wave angle ( $\alpha_m = 0.4$  rad,  $\gamma L = 1$ )

91. The solution obtained for a variable breaking wave angle overestimates the rate of erosion behind the jetty since it is assumed that the amplitude of the longshore sand transport rate is everywhere the same (and thus that the wave height, in principle, is constant). In reality, diffraction reduces the wave height in the shadow region and, accordingly, the amplitude of the longshore sand transport rate there. Despite this reduction, Equations 103 and 104 provide a better description of the actual situation than the commonly used solution (Equation 64) for which maximum erosion will always appear immediately adjacent to the jetty or long groin.

## REFERENCES

- Abramowitz, M., and Stegun, I. 1965. Handbook of Mathematical Functions with Formulas, Graphs and Mathematical Tables, Dover Publications, New York, NY.
- Bakker, W. T. 1969. "The Dynamics of a Coast with a Groin System," Proceedings of the 11th Coastal Engineering Conference, American Society of Civil Engineers, pp 492-517.
- \_\_\_\_\_. 1970. "The Influence of Diffraction near a Harbour Mole on the Coastal Shape," Rijkswaterstaat Directie Waterhuishouding en Waterbeweging, afd Kustonderzoek, Rapport W. W. K. 70-2 (in Dutch).
- Bakker, W. T., and Edelman, T. 1965. "The Coastline of River Deltas," Proceedings of the 9th Coastal Engineering Conference, American Society of Civil Engineers, pp 199-218.
- Bakker, W. T., Klein-Breteler, E. H. J., and Roos, A. 1971. "The Dynamics of a Coast with a Groin System," Proceedings of the 12th Coastal Engineering Conference, American Society of Civil Engineers, pp 1001-1020.
- Carslaw, H., and Jaeger, J. 1959. Conduction of Heat in Solids, Clarendon Press, Oxford.
- Crank, J. 1975. The Mathematics of Diffusion, 2nd ed., Clarendon Press, Oxford.
- Dean, R. G. 1973. "Heuristic Models of Sand Transport in the Surf Zone," Proceedings of the Australian Conference on Coastal Engineering, pp 208-214.
- \_\_\_\_\_. 1984. CRC Handbook of Coastal Processes and Erosion, Komar, P. D., editor, CRC Press Inc., Boca Raton, Fla.
- Erdelyi, A., Magnus, W., Oberhettinger, F., and Tricomi, F. 1954. "Tables of Integral Transforms," Vol 1, McGraw-Hill, New York, NY, 391 pp.
- Grijm, W. 1961. "Theoretical Forms of Shoreline," Proceedings of the 7th Coastal Engineering Conference, American Society of Civil Engineers, pp 197-202.
- \_\_\_\_\_. 1965. "Theoretical Forms of Shoreline," Proceedings of the 9th Coastal Engineering Conference, American Society of Civil Engineers, pp 219-235.
- Hanson, H., and Kraus, N. C. 1986. "Seawall Boundary Condition in Numerical Models of Shoreline Evolution," Technical Report CERC-86-3, US Army Engineer Waterways Experiment Station, Vicksburg, Miss.
- Komar, P. D. 1973. "Computer Models of Delta Growth Due to Sediment Input from Waves and Longshore Transport," Geological Society of America Bulletin, Vol 84, pp 2217-2226.

- Kraus, N. C. 1983. "Applications of a Shoreline Prediction Model," Proceedings of Coastal Structures '83, American Society of Civil Engineers, pp 632-645.
- Kraus, N. C., and Harikai, S. 1983. "Numerical Model of the Shoreline Change at Oarai Beach," Coastal Engineering, Vol 7, No. 1, pp 1-28.
- Le Méhauté, B., and Brebner, A. 1961. "An Introduction to Coastal Morphology and Littoral Processes," Report No. 14, Civil Engineering Department, Queens University at Kingston, Ontario, Canada.
- Le Méhauté, B., and Soldate, M. 1977. "Mathematical Modeling of Shoreline Evolution," CERC Miscellaneous Report No. 77-10, US Army Engineer Waterways Experiment Station, Vicksburg, Miss.
- \_\_\_\_\_. 1978. "Mathematical Modeling of Shoreline Evolution," Report No. TC-831, Tetra Tech, Inc., Pasadena, Calif.
- \_\_\_\_\_. 1979. "Mathematical Modeling of Shoreline Evolution," Proceedings of the 16th Coastal Engineering Conference, American Society of Civil Engineers, pp 1163-1179.
- Longuet-Higgins, M. S. 1970a. "Longshore Currents Generated by Obliquely Incident Sea Waves, 1," Journal of Geophysical Research, Vol 75, No. 33, pp 6778-6789.
- \_\_\_\_\_. 1970b. "Longshore Currents Generated by Obliquely Incident Sea Waves, 2," Journal of Geophysical Research, Vol 75, No. 33, pp 6790-6801.
- Pelnard-Considère, R. 1956. "Essai de Théorie de l'Evolution des Forms de Rivages en Plage de Sable et de Galets," 4th Journées de l'Hydraulique, les Energies de la Mer, Question III, Rapport No. 1, pp 289-298.
- Shore Protection Manual. 1984. 4th ed., 2 vols, US Army Engineer Waterways Experiment Station, Coastal Engineering Research Center, US Government Printing Office, Washington, DC.
- Walton, T., and Chiu, T. 1979. "A Review of Analytical Techniques to Solve the Sand Transport Equation and Some Simplified Solutions," Proceedings of Coastal Structures '79, American Society of Civil Engineers, pp 809-837.

APPENDIX A: A SHORT INTRODUCTION TO THE LAPLACE  
TRANSFORM TECHNIQUE

1. The Laplace transform is a powerful technique for solving linear partial differential equations. This technique allows the target partial differential equation to be converted to an ordinary linear differential equation in the transformed plane for solving one-dimensional problems in space. The Laplace transform of a function  $y$  is denoted as  $L\{y\}$  and is defined by the operation:

$$L\{y\} = \bar{y} = \int_0^{\infty} y(x,t) e^{-st} dt \quad (A1)$$

The over bar denotes the transformed function. The transform of a derivative of a function with respect to time is

$$L\left\{\frac{\partial y}{\partial t}\right\} = s\bar{y} - y(x,0) \quad (A2)$$

This relationship may be derived by performing a partial integration of Equation A1. The term  $y(x,0)$  represents the initial conditions for the system. Accordingly, the transform of the diffusion equation may be written (if, with the convention  $y(x,0) = 0$ , that is, a shoreline which is initially parallel to the x-axis):

$$\frac{d^2\bar{y}}{dx^2} - \frac{s}{\epsilon}\bar{y} = 0 \quad (A3)$$

The general solution of this homogeneous linear differential equation is

$$\bar{y} = Ae^{qx} + Be^{-qx} \quad (A4)$$

where

$$q^2 = \frac{s}{\epsilon}$$

2. The coefficients  $A$  and  $B$  are determined by the transformed boundary conditions and are, in general, functions of the parameter  $s$ . To obtain a solution in the time domain, Equation A4 has to be inverse transformed. This can be accomplished using tables of known transforms (see, for example, Erdelyi et al. (1954) and Abramowitz and Stegun (1965))\* or the Fourier inversion theorem which states

$$y = \frac{1}{2\pi i} \int_{\zeta-i\infty}^{\zeta+i\infty} e^{st} \bar{y}(s) ds \quad (A5)$$

The integration is performed as a line integral in the complex plane, for which  $\zeta$  is taken sufficiently large to have all singularities of the function  $\bar{y}(s)$  lying to the left. Equation A5 is normally evaluated by means of the residue calculus. If several solution areas are used, the solution within each area is of the form of Equation A4. The solutions are dependent upon each other through their common boundaries (as an example see Appendix E) by the prevailing boundary conditions.

3. Table A1 presents a short summary of selected applicable transforms useful for solving the diffusion equation.

---

\* References cited in the Appendix can be found in the References at the end of the main text.

Table A1  
Short Table of Laplace Transforms of Functions Often  
Encountered in Solving the Diffusion Equation

| $\bar{y}(s)$                 | $y(t)$  |
|------------------------------|---|
| $\frac{e^{-qx}}{q}$          | $\left(\frac{\epsilon}{\pi t}\right)^{1/2} e^{-x^2/4\epsilon t}$  |
| $\frac{e^{-qx}}{s}$          | $\operatorname{erfc}\left(\frac{x}{2\sqrt{\epsilon t}}\right)$  |
| $\frac{e^{-qx}}{qs}$         | $2\left(\frac{\epsilon t}{\pi}\right)^{1/2} e^{-x^2/4\epsilon t} - x \operatorname{erfc}\left(\frac{x}{2\sqrt{\epsilon t}}\right)$  |
| $\frac{e^{-qx}}{s^{1+1/2n}}$ | $(4t)^{1/2n} i^n \operatorname{erfc}\left(\frac{x}{2\sqrt{\epsilon t}}\right)$  |
| $n = 0, 1, 2, \dots$         |   |
| $\frac{e^{-qx}}{q+h}$        | $\left(\frac{\epsilon}{\pi t}\right)^{1/2} e^{-x^2/4\epsilon t} - h e^{\epsilon h^2 t} \operatorname{erfc}\left[\frac{x}{2\sqrt{\epsilon t}} + h\sqrt{\epsilon t}\right]$   |
| $\frac{e^{-qx}}{qs(q+h)}$    | $\frac{2}{h}\left(\frac{\epsilon t}{\pi}\right)^{1/2} e^{-x^2/4\epsilon t} - \left(\frac{1+hx}{h^2}\right) \operatorname{erfc}\left(\frac{x}{2\sqrt{\epsilon t}}\right) + \frac{1}{h^2} e^{\epsilon h^2 t} \operatorname{erfc}\left(\frac{x}{2\sqrt{\epsilon t}} + h\sqrt{\epsilon t}\right)$ |

$h$  is an unrestricted constant





APPENDIX B: SHORELINE EVOLUTION DOWNDRIIFT OF A GROIN WITH  
BYPASSING REPRESENTED BY AN EXPONENTIAL FUNCTION

1. Sand is transported past the groin according to the following relationship:

$$Q = Q_B(1 - e^{-\gamma t}) \quad (B1)$$

Here  $Q_B$  denotes the maximum bypassing sand transport rate which occurs at the groin, and  $\gamma$  is a rate coefficient describing the rate at which the limiting value  $Q_B$  is approached in time. Using Equation 8, the boundary condition at the groin is written:

$$\frac{\partial y}{\partial x} = \alpha_0 - \frac{1}{2} \frac{Q_B}{Q_0} (1 - e^{-\gamma t}) \quad x = 0 \quad (B2)$$

Consequently, the mathematical statement of this case is, together with the above boundary condition:

$$\epsilon \frac{\partial^2 y}{\partial x^2} = \frac{\partial y}{\partial t} \quad (B3)$$

$$y(x, t) = 0 \quad x \rightarrow \infty \quad (B4)$$

$$y(x, 0) = 0 \quad (B5)$$

2. By using the Laplace transform technique, an ordinary linear differential equation is obtained:

$$\frac{d^2 \bar{y}}{dx^2} - \frac{s}{\epsilon} \bar{y} = 0 \quad (B6)$$

where  $\bar{y}$  denotes the transformed function of  $y$ . The transformed boundary condition is

$$\frac{d\bar{y}}{dx} = \frac{\alpha_o}{s} - \frac{1}{2} \frac{Q_B}{Q_o} \left( \frac{1}{s} - \frac{1}{s + \gamma} \right) \quad (B7)$$

Solving Equation B6 together with Equations B4 and B7 yields

$$\bar{y} = - \left( \alpha_o - \frac{1}{2} \frac{Q_B}{Q_o} \right) \frac{e^{-qx}}{qs} - \frac{1}{2} \frac{Q_B}{Q_o} \frac{e^{-qx}}{q(s + \gamma)} \quad (B8)$$

where  $q^2 = \frac{s}{\epsilon}$

3. The inverse Laplace transform of the first term in Equation B8 is found to be (Appendix A)

$$y^1 = - \left( \alpha_o - \frac{1}{2} \frac{Q_B}{Q_o} \right) \left( 2 \sqrt{\frac{\epsilon t}{\pi}} e^{-x^2/4\epsilon t} - x \operatorname{erfc} \frac{x}{2\sqrt{\epsilon t}} \right) \quad (B9)$$

The second term is evaluated by applying Duhamel's theorem (Carslaw and Jaeger 1959, p. 301) which reads

$$L \left\{ \int_0^t f_1(\tau) f_2(t - \tau) d\tau \right\} = L\{f_1(t)\} L\{f_2(t)\} \quad (B10)$$

in which  $L\{\}$  represents the Laplace transform operation. The second term of Equation B8 yields, after some rearranging,

$$y^2 = - \frac{Q_B}{Q_o} \sqrt{\frac{\epsilon}{\pi}} e^{-\gamma t} \int_0^{\sqrt{t}} e^{\gamma \xi^2 - x^2/4\epsilon \xi^2} d\xi \quad (B11)$$

Accordingly, the complete solution is

$$y(x,t) = - \left( \alpha_o - \frac{1}{2} \frac{Q_B}{Q_o} \right) \left[ 2 \sqrt{\frac{\epsilon t}{\pi}} e^{-x^2/4\epsilon t} - x \operatorname{erfc} \left( \frac{x}{2\sqrt{\epsilon t}} \right) \right]$$

$$- \frac{Q_B}{Q_o} \sqrt{\frac{\epsilon}{\pi}} e^{-\gamma t} \int_0^{\sqrt{t}} e^{\gamma \xi^2 - x^2/4\epsilon \xi^2} d\xi \quad (\text{B12})$$

4. The last term on the right side of Equation B12 describes a transient which disappears with time. After the effect of the transient term has vanished, the solution for shoreline change downdrift of a groin will be the same as the solution obtained without bypassing but with a modified breaking wave angle. If  $Q_B < 2Q_o \alpha_o$  erosion will take place; whereas if  $Q_B > 2Q_o \alpha_o$  there will be accretion.



APPENDIX C: SHORELINE EVOLUTION BEHIND A DETACHED BREAKWATER

1. In Figure 35 (in the main text) a definition sketch is shown for the case of a detached breakwater and normal incident waves. The shoreline evolution is symmetric about the centerline of the detached breakwater; thus, only half of the problem domain needs to be considered. Since the amplitude of the sand transport rate  $Q_o$  and the incident breaking wave angle  $\alpha_o$  are different behind the breakwater and outside the breakwater, two solution areas are required. Mathematically, the shoreline evolution is described by Equations 74-79. After the Laplace transform technique is applied, the following system of ordinary linear differential equations is obtained:

$$\frac{d^2 \bar{y}_1}{dx^2} - \frac{s}{\epsilon_1} \bar{y}_1 = 0 \quad -L \leq x \leq 0 \quad (C1)$$

$$\frac{d^2 \bar{y}_2}{dx^2} - \frac{s}{\epsilon_2} \bar{y}_2 = 0 \quad x > 0 \quad (C2)$$

$$\frac{d\bar{y}_1}{dx} = \frac{\tan \alpha_{o1}}{s} \quad x = -L \quad (C3)$$

$$\bar{y}_2 = 0 \quad x \rightarrow \infty \quad (C4)$$

$$\bar{y}_1 = \bar{y}_2 \quad x = 0 \quad (C5)$$

$$\frac{d\bar{y}_1}{dx} = \frac{Q_{o2}}{Q_{o1}} \frac{d\bar{y}_2}{dx} + \frac{\alpha_{o1}}{s} \quad (C6)$$

in which  $\bar{y}_1$  and  $\bar{y}_2$  denote the transformed shoreline position corresponding to the regions behind and outside the breakwater, respectively, and  $L$  is half the length of the breakwater. Solving the system of equations subject to the boundary conditions yields

$$\bar{y}_1 = -\frac{\delta\alpha_{o1}}{\delta+1} \frac{e^{q_1 x}}{q_1 s} + \left[ \delta \cosh(q_1 x) - \sinh(q_1 x) \right] \frac{\left( \tan \alpha_{o1} - \frac{\delta\alpha_{o1}}{\delta+1} e^{-q_1 L} \right)}{q_1 s (\delta \sinh q_1 L + \cosh q_1 L)} \quad -L \leq x \leq 0 \quad (C7)$$

$$\bar{y}_2 = -\frac{\delta\alpha_{o1}}{\delta+1} \frac{e^{-q_2 x}}{q_1 s} + \frac{\left( \tan \alpha_{o1} - \frac{\delta\alpha_{o1}}{\delta+1} e^{-q_1 L} \right) \delta e^{-q_2 x}}{q_1 s (\delta \sinh q_1 L + \cosh q_1 L)} \quad x > 0 \quad (C8)$$

where

$$\delta^2 = \frac{Q_{o1}}{Q_{o2}} \quad q_1^2 = \frac{s}{\varepsilon_1} \quad q_2^2 = \frac{s}{\varepsilon_2} \quad (C9)$$

2. The inverse transform of Equations C7 and C8 may be obtained by use of the Fourier inversion theorem (Appendix A) or by expanding the denominator in a Taylor series and finding the inverse transform of each term in the series. The latter method will be used here. The denominator may be rewritten as

$$q_1 s (\delta \sinh q_1 L + \cosh q_1 L) = \frac{1}{2} q_1 s e^{q_1 L} (\delta + 1) \left[ 1 - \left( \frac{\delta - 1}{\delta + 1} \right) e^{-2q_1 L} \right] \quad (C10)$$

The last term in Equation C10 is expanded in a Taylor series according to

$$\left[ 1 - \left( \frac{\delta - 1}{\delta + 1} \right) e^{-2q_1 L} \right]^{-1} = \sum_{n=0}^{\infty} \left( \frac{\delta - 1}{\delta + 1} \right)^n e^{-2q_1 n L} \quad (C11)$$

3. Only the inverse transform of Equation C8 will be obtained here to illustrate the procedure. The inverse transform of the first term in Equation C8 is (noting that  $q_2 = \delta q_1$ )

$$y_2^1 = -\frac{\delta \alpha_{01}}{\delta + 1} 2\sqrt{\epsilon_1 t} \operatorname{ierfc} \left( \frac{\delta x}{\sqrt{2\epsilon_1 t}} \right) \quad (\text{C12})$$

in which the function  $\operatorname{ierfc}$  is defined according to Equation 23. The second part of Equation C8 is rewritten by using Equation C11:

$$\bar{y}_2^{-2} = 2 \frac{\delta}{\delta + 1} \left( \tan \alpha_{01} - \frac{\delta \alpha_{01}}{\delta + 1} e^{-q_1 L} \right) \frac{e^{-q_1(\delta x + L)}}{q_1 s} \sum_{n=0}^{\infty} \left( \frac{\delta - 1}{\delta + 1} \right)^n e^{-2q_1 n L} \quad (\text{C13})$$

Rearranging Equation C13 by moving terms inside the summation gives

$$\begin{aligned} \bar{y}_2^{-2} = 2 \frac{\delta \tan \alpha_{01}}{\delta + 1} \sum_{n=0}^{\infty} \left\{ \frac{\left( \frac{\delta - 1}{\delta + 1} \right)^n e^{-q_1 [L(2n+1) + \delta x]}}{q_1 s} \right\} \\ - 2 \frac{\delta^2 \alpha_{01}}{(\delta + 1)^2} \sum_{n=0}^{\infty} \left\{ \frac{\left( \frac{\delta - 1}{\delta + 1} \right)^n e^{-q_1 [2L(n+1) + \delta x]}}{q_1 s} \right\} \end{aligned} \quad (\text{C14})$$

This expression is inverse transformed term by term (Appendix A). The solution is

$$\begin{aligned} y_2^2 = 2 \frac{\delta \tan \alpha_{01}}{\delta + 1} \sum_{n=0}^{\infty} \left\{ \left( \frac{\delta - 1}{\delta + 1} \right)^n 2\sqrt{\epsilon_1 t} \operatorname{ierfc} \left[ \frac{\delta x + L(2n + 1)}{2\sqrt{\epsilon_1 t}} \right] \right\} \\ - 2 \frac{\delta^2 \alpha_{01}}{(\delta + 1)^2} \sum_{n=0}^{\infty} \left\{ \left( \frac{\delta - 1}{\delta + 1} \right)^n 2\sqrt{\epsilon_1 t} \operatorname{ierfc} \left[ \frac{\delta x + 2L(n + 1)}{2\sqrt{\epsilon_1 t}} \right] \right\} \end{aligned} \quad (\text{C15})$$

The complete solution to Equation C8 is written as

$$\begin{aligned}
 y_2 = & - \frac{\delta \alpha_{o1}}{\delta + 1} 2\sqrt{\epsilon_1 t} \operatorname{ierfc} \left( \frac{\delta x}{2\sqrt{\epsilon_1 t}} \right) \\
 & + 2 \frac{\delta \tan \alpha_{o1}}{\delta + 1} \sum_{n=0}^{\infty} \left\{ \left( \frac{\delta - 1}{\delta + 1} \right)^n 2\sqrt{\epsilon_1 t} \operatorname{ierfc} \left[ \frac{\delta x + L(2n + 1)}{2\sqrt{\epsilon_1 t}} \right] \right\} \\
 & - 2 \frac{\delta^2 \alpha_{o1}}{(\delta + 1)^2} \sum_{n=0}^{\infty} \left\{ \left( \frac{\delta - 1}{\delta + 1} \right)^n 2\sqrt{\epsilon_1 t} \operatorname{ierfc} \left[ \frac{\delta x + 2L(n + 1)}{2\sqrt{\epsilon_1 t}} \right] \right\} \quad (C16)
 \end{aligned}$$

In the same way, Equation C7 may be inverse transformed, resulting in Equation 81 (main text).



APPENDIX D: SHORELINE EVOLUTION IN THE VICINITY OF A SEAWALL  
WHERE FLANKING OCCURS

1. Two solution areas are employed to describe flanking of a semi-infinite seawall, one area behind the seawall and the other away from the seawall. The amplitudes of the sand transport rate are denoted as  $Q_{o1}$  and  $Q_{o2}$  in the respective solution areas, and the corresponding incident breaking wave angles are denoted as  $\alpha_{o1}$  and  $\alpha_{o2}$ . The incident breaking wave angle  $\alpha_{o1}$  behind the seawall (solution area 1) should be interpreted as a representative mean value related to the sand transport rate. Equations 84-89 (main text) constitute the mathematical formulation of shoreline evolution in the vicinity of a seawall subject to flanking. The Laplace transformed system of equations and the boundary conditions are

$$\frac{d^2 \bar{y}_1}{dx^2} - \frac{s}{\epsilon_1} \bar{y}_1 = 0 \quad x \leq 0 \quad (D1)$$

$$\frac{d^2 \bar{y}_2}{dx^2} - \frac{s}{\epsilon_2} \bar{y}_2 = 0 \quad x > 0 \quad (D2)$$

$$\bar{y}_1 = 0 \quad x \rightarrow -\infty \quad (D3)$$

$$\bar{y}_2 = 0 \quad x \rightarrow \infty \quad (D4)$$

$$\bar{y}_1 = \bar{y}_2 \quad x = 0 \quad (D5)$$

$$\frac{d\bar{y}_1}{dx} = \frac{1}{\delta^2} \frac{d\bar{y}_2}{dx} + \left( \alpha_{o1} - \frac{1}{\delta^2} \alpha_{o2} \right) \frac{1}{s} \quad x = 0 \quad (D6)$$

2. Solving the system of ordinary linear differential equations subject to the boundary conditions yields

$$\bar{y}_1 = \frac{\alpha_{o1} - \frac{1}{\delta^2} \times \alpha_{o2}}{1 + \frac{1}{\delta}} \frac{e^{q_1 x}}{q_1 s} \quad x \leq 0 \quad (D7)$$

$$\bar{y}_2 = \frac{\alpha_{o1} - \frac{1}{\delta^2} \times \alpha_{o2}}{1 + \frac{1}{\delta}} \frac{e^{-q_1 \delta x}}{q_1 s} \quad x > 0 \quad (D8)$$

3. The inverse transforms of Equations D7 and D8 are (Appendix A):

$$y_1 = \frac{\delta^2 \alpha_{o1} - \alpha_{o2}}{\delta(\delta + 1)} \left[ 2 \sqrt{\frac{\epsilon_1 t}{\pi}} e^{-x^2/4\epsilon_1 t} + x \operatorname{erfc} \left( \frac{-x}{2\sqrt{\epsilon_1 t}} \right) \right] \quad (D9)$$

$$x \leq 0$$

$$y_2 = \frac{\delta^2 \alpha_{o1} - \alpha_{o2}}{\delta(\delta + 1)} \left[ 2 \sqrt{\frac{\epsilon_1 t}{\pi}} e^{-\delta^2 x^2/4\epsilon_1 t} - \delta x \operatorname{erfc} \left( \frac{\delta x}{2\sqrt{\epsilon_1 t}} \right) \right] \quad (D10)$$

$$x > 0$$

APPENDIX E: SHORELINE EVOLUTION DOWNDRIIFT OF A JETTY IF AN ARBITRARY NUMBER OF SOLUTION AREAS IS USED TO MODEL DIFFRACTION

1. The area downdrift of a jetty is divided into N distinct solution areas of assumed different sand transport properties. In an arbitrary solution area j, the amplitude of sand transport rate is denoted as  $Q_{oj}$  and the incident breaking wave angle as  $\alpha_{oj}$ . The shoreline evolution is denoted as  $y_j$  in the solution area bounded by the shoreline coordinates  $x_j$  and  $x_{j+1}$ . Equations 95 to 99 (main text) mathematically describe the shoreline evolution in one solution area. Using the Laplace transform technique, the governing equations take the following form:

$$\frac{d^2 \bar{y}_j}{dx^2} - \frac{s}{\epsilon_j} \bar{y}_j = 0 \quad (E1)$$

$$\bar{y}_j = \bar{y}_{j+1} \quad x = x_{j+1} \quad (E2)$$

$$\bar{y}_j = \bar{y}_{j-1} \quad x = x_j \quad (E3)$$

$$\frac{d\bar{y}_j}{dx} = \delta_{j-1}^2 \frac{d\bar{y}_{j-1}}{dx} + \left( \alpha_{oj} - \delta_{j-1}^2 \alpha_{oj-1} \right) \frac{1}{s} \quad (E4)$$

$$x = x_j$$

$$\frac{d\bar{y}_{j+1}}{dx} = \delta_j^2 \frac{d\bar{y}_j}{dx} + \left( \alpha_{oj+1} - \delta_j^2 \alpha_{oj} \right) \frac{1}{s} \quad (E5)$$

$$x = x_{j+1}$$

where

$$\delta_j^2 = \frac{Q_{oj}}{Q_{oj+1}} \quad (E6)$$

The solution to the ordinary linear differential Equation E1 is

$$\bar{y}_j = A_j e^{q_j x} + B_j e^{-q_j x} \quad (E7)$$

where

$$q_j^2 = \frac{s}{\epsilon_j} \quad (E8)$$

in which  $A_j$  and  $B_j$  are constants to be determined through the boundary conditions. Since the shoreline evolution in each solution area is connected via the boundary conditions with the neighboring areas, an equation system with  $2N$  unknowns (two constants for every solution area) is obtained. The boundary conditions E2 and E3 give the following relationships:

$$A_j e^{q_j x_j} + B_j e^{-q_j x_j} = A_{j-1} e^{q_{j-1} x_j} + B_{j-1} e^{-q_{j-1} x_j} \quad (E9)$$

$$A_j e^{q_j x_{j+1}} + B_j e^{-q_j x_{j+1}} = A_{j+1} e^{q_{j+1} x_{j+1}} + B_{j+1} e^{-q_{j+1} x_{j+1}} \quad (E10)$$

2. Furthermore, Equations E4 and E5 give

$$A_j e^{q_j x_j} - B_j e^{-q_j x_j} = \delta_{j-1} A_{j-1} e^{q_{j-1} x_j} - \delta_{j-1} B_{j-1} e^{-q_{j-1} x_j} + \frac{\beta_{j-1}}{q_j s} \quad (E11)$$

$$A_{j+1} e^{q_{j+1} x_{j+1}} - B_{j+1} e^{-q_{j+1} x_{j+1}} = \delta_j A_j e^{q_j x_{j+1}} - \delta_j B_j e^{-q_j x_{j+1}} + \frac{\beta_j}{q_{j+1}^s} \quad (E12)$$

where

$$\beta_j = \alpha_{oj+1} - \delta_j^2 \alpha_{oj} \quad (E13)$$

3. Equations similar to E9 to E13 may be written from solution area 2 to solution area N-1. In the first and last solution areas, two other conditions prevail at the outer boundaries, namely, no sand transport in the first solution area (area 1) and no shoreline change as  $x \rightarrow \infty$  in the last solution area (area N). The Laplace transforms of these boundary conditions are

$$\frac{d\bar{y}_1}{dx} = \tan \alpha_{o1} \quad x = 0 \quad (E14)$$

$$\bar{y}_N = 0 \quad x \rightarrow \infty \quad (E15)$$

4. Equation E15 implies that the constant  $A_N$  is zero. The resulting system of equations to be solved in order to determine the value of the constants is conveniently written in matrix form. A general system of N solution areas gives rise to  $2N - 1$  equations as follows:

$$\begin{bmatrix} 1 & -1 & 0 & 0 & 0 & 0 & \dots & 0 \\ e^{q_1 x_2} & e^{-q_1 x_2} & -e^{q_2 x_2} & -e^{-q_2 x_2} & 0 & 0 & \dots & 0 \\ -\delta_1 e^{q_1 x_2} & \delta_1 e^{-q_1 x_2} & e^{q_2 x_2} & -e^{-q_2 x_2} & 0 & 0 & \dots & 0 \\ 0 & 0 & e^{q_2 x_3} & -e^{-q_2 x_3} & -e^{q_3 x_3} & -e^{-q_3 x_3} & \dots & 0 \\ \vdots & & & & & & & \vdots \\ 0 & \dots & & & & & & 0 \\ 0 & \dots & & e^{q_{N-1} x_N} & -e^{-q_{N-1} x_N} & -e^{q_N x_N} & & \\ 0 & \dots & & -\delta_{N-1} e^{q_{N-1} x_N} & \delta_{N-1} e^{-q_{N-1} x_N} & -e^{q_N x_N} & & \end{bmatrix} \cdot \begin{bmatrix} A_1 \\ B_1 \\ A_2 \\ B_2 \\ \vdots \\ A_{N-1} \\ B_{N-1} \\ B_N \end{bmatrix} = \begin{bmatrix} \frac{\tan \alpha_{o1}}{q_1^s} \\ 0 \\ \frac{\beta_1}{q_2^s} \\ 0 \\ \vdots \\ \frac{\beta_{N-2}}{q_{N-1}^s} \\ 0 \\ \frac{\beta_{N-1}}{q_N^s} \end{bmatrix} \quad (E16)$$

It is seen that the solution corresponding to even a small number of solution areas involves intensive algebraic calculations. Furthermore, the inverse transformation is difficult to perform, necessitating use of the Fourier inversion theorem.

APPENDIX F: SHORELINE EVOLUTION BEHIND A JETTY FOR  
LINEARLY VARYING BREAKING WAVE ANGLE

1. In the case of shoreline evolution behind a jetty for linearly varying breaking wave angle, the amplitude of the sand transport rate is regarded as constant downdrift of the jetty, and the incident breaking wave angle varies linearly from the jetty (with value  $\alpha_v$ ) to the value  $\alpha_H$  in the region undisturbed by the jetty. Two solution areas are needed for describing shoreline change, one in the shadow region and the other outside the shadow region (illuminated area). Equation 101 (main text) describes the variation in breaking wave angle in the shadow region which is of length  $B$ . The Laplace transformed equations and boundary conditions are

$$\frac{d^2 \bar{y}_1}{dx^2} - \frac{s}{\epsilon} \bar{y}_1 = \frac{\alpha_H - \alpha_v}{B} \frac{1}{s} \quad 0 \leq x \leq B \quad (F1)$$

$$\frac{d^2 \bar{y}_2}{dx^2} - \frac{s}{\epsilon} \bar{y}_2 = 0 \quad x > B \quad (F2)$$

$$\frac{d\bar{y}_1}{dx} = \frac{\tan \alpha_v}{s} \quad x = 0 \quad (F3)$$

$$\bar{y}_1 = \bar{y}_2 \quad x = B \quad (F4)$$

$$\frac{d\bar{y}_1}{dx} = \frac{d\bar{y}_2}{dx} \quad x = B \quad (F5)$$

2. The solution to this system of ordinary linear differential equations is

$$\bar{y}_1 = \left( \frac{\alpha_H - \alpha_v}{2B} \right) \epsilon \left[ \frac{e^{-q(B-x)}}{s^2} + \frac{e^{-q(B+x)}}{s^2} - \frac{2}{s^2} \right] - \frac{\tan \alpha_v e^{-qx}}{qs} \quad (F6)$$

$$\bar{y}_2 = \left( \frac{\alpha_H - \alpha_v}{2B} \right) \epsilon \left[ \frac{e^{-q(x+B)}}{s^2} - \frac{e^{-q(x-B)}}{s^2} \right] - \tan \alpha \frac{e^{-qx}}{v qs} \quad (F7)$$

where

$$q^2 = \frac{s}{\epsilon} \quad (F8)$$

3. Equations F6 and F7 are easily transformed term by term (see Appendix A) to yield Equations 103 and 104 (main text).



APPENDIX G: SHORELINE EVOLUTION BEHIND A JETTY FOR EXPONENTIALLY VARYING BREAKING WAVE ANGLE

1. The breaking wave angle varies exponentially with the distance behind the jetty from zero at the jetty to the undisturbed value  $\alpha_m$  far from the jetty. The mathematical formulation of the boundary condition at the jetty is expressed by Equation 105 (main text). A varying breaking wave angle along the x-axis is described in terms of the diffusion equation by a distributed sink with a decaying strength with distance. The transformed equation and boundary conditions are

$$\frac{d^2 \bar{y}}{dx^2} - \frac{s}{\epsilon} \bar{y} = \frac{\alpha_m \gamma}{s} e^{-\gamma x} \quad x \geq 0 \quad (G1)$$

$$\frac{d\bar{y}}{dx} = 0 \quad x = 0 \quad (G2)$$

$$\bar{y} = 0 \quad x \rightarrow \infty \quad (G3)$$

The solution to Equation G1 is

$$\bar{y} = -\frac{\alpha_m \gamma^2 e^{-qx}}{qs(\gamma^2 - q^2)} + \frac{\alpha_m \gamma e^{-\gamma x}}{s(\gamma^2 - q^2)} \quad (G4)$$

Equation G4 may be written as partial fractions:

$$\bar{y} = \frac{\alpha_m \gamma e^{-qx}}{2qs} \left( \frac{1}{q - \gamma} - \frac{1}{q + \gamma} \right) - \frac{\alpha_m e^{-\gamma x}}{\gamma} \left( \frac{1}{s - \gamma^2 \epsilon} - \frac{1}{s} \right) \quad (G5)$$

In Equation G5, the last term may be inverse transformed to yield

$$y^2 = \frac{\alpha_m e^{-\gamma x}}{\gamma} \left( 1 - e^{\gamma^2 \epsilon t} \right) \quad (G6)$$

2. The first part of the first term is inverse transformed according to Appendix A and gives

$$y^{1a} = \frac{\alpha_m \gamma}{2} \left[ -\frac{2}{\gamma} \sqrt{\frac{\epsilon t}{\pi}} e^{-x^2/4\epsilon t} - \left( \frac{1 - \gamma x}{\gamma^2} \right) \operatorname{erfc} \left( \frac{x}{2\sqrt{\epsilon t}} \right) + \frac{1}{2} e^{-\gamma x + \epsilon t \gamma^2} \operatorname{erfc} \left( \frac{x}{2\sqrt{\epsilon t}} - \gamma\sqrt{\epsilon t} \right) \right] \quad (G7)$$

In the same way, the inverse transform of the second part of the first term in Equation G5 gives

$$y^{1b} = \frac{\alpha_m \gamma}{2} \left[ \frac{2}{\gamma} \sqrt{\frac{\epsilon t}{\pi}} e^{-x^2/4\epsilon t} - \left( \frac{1 + \gamma x}{\gamma^2} \right) \operatorname{erfc} \left( \frac{x}{2\sqrt{\epsilon t}} \right) + \frac{1}{2} e^{\gamma x + \epsilon t \gamma^2} \operatorname{erfc} \left( \frac{x}{2\sqrt{\epsilon t}} + \gamma\sqrt{\epsilon t} \right) \right] \quad (G8)$$

3. The complete solution consists of Equations G6, G7, and G8 as given by Equation 106 (main text).

APPENDIX H: NOTATION

|          |  |
|----------|--|
| a        | Length (m)   |
| A        | Amplitude of periodic beach cusps (m)  |
| A        | Cross-sectional periodic beach area ( $m^2$ )  |
| A, B     | Constants in general functions of the Laplace transform variable   |
| B        | Length of shadow region downdrift of a groin (m)   |
| $Cg_b$   | Wave group velocity to breaking point (m/sec)  |
| D        | Depth of closure (m)   |
| erf      | Error function   |
| f(x)     | Arbitrary initial shoreline shape (m)  |
| g        | Acceleration of gravity ( $m^2/sec$ )  |
| h        | Constant   |
| $H_{sb}$ | Significant breaking wave height (m)   |
| i        | Integer number   |
| ierfc    | Integral of the error function   |
| k        | Slope of a line segment  |
| K        | Nondimensional constant  |
| L        | Geometric length (m)   |
| L{y}     | Laplace transform of a function y  |
| $L_o$    | Nondimensional groin length  |
| m        | Integer number   |
| n        | Integer number   |
| N        | Number of solution areas or reaches  |
| p        | Pitch height of a circle segment (m)   |
| P        | Loss percentage from a beach fill  |
| q        | Sand transport rate per unit length of beach from a source or sink ( $m^3/m/sec$ )   |
| $q_o$    | Constant sand discharge from a river acting as a point source ( $m^3/sec$ )  |
| $q_R$    | Time variable sand discharge from a river acting as a point source ( $m^3/sec$ ); constant sand discharge from a river with a finite mouth ( $m^3/m/sec$ ) |
| $q_s$    | Amplitude of sand discharge from a river acting as a point source ( $m^3/sec$ )  |
| $q^2$    | $s/\epsilon$   |

|            |  |
|------------|--|
| Q          | Longshore sand transport rate ( $m^3/sec$ )  |
| $Q_B$      | Maximum value of bypassing sand transport rate ( $m^3/sec$ )   |
| $Q_o$      | Amplitude of longshore sand transport rate ( $m^3/sec$ )   |
| s          | Laplace transform variable   |
| t          | Time (sec)   |
| $t'$       | Dimensionless time   |
| $t_G$      | Time when bypassing of a groin starts (sec)  |
| $t_p$      | Time (sec)   |
| $t_s$      | Time (s)   |
| $t_v$      | Time in the matching solution when groin bypassing starts (sec)  |
| $t_*$      | Modified time in matching solution (sec)   |
| T          | Time period of an oscillation (sec)  |
| V          | Volume of sand released from an instantaneous source ( $m^3$ )   |
| W          | Distance between two groins (compartment length) (m)   |
| x          | Space coordinate along axis parallel to trend of shoreline (m)   |
| $x'$       | Dimensionless alongshore distance  |
| $x_s$      | Distance alongshore (m)  |
| $\bar{y}$  | Laplace transform of a function y  |
| y          | Shoreline position (m)   |
| $y'$       | Dimensionless shoreline position   |
| $y_o$      | Geometric length   |
| z          | Integration variable   |
| $\alpha$   | Angle  |
| $\alpha_b$ | Angle between breaking wave crests and shoreline   |
| $\alpha_o$ | Angle between breaking wave crests and coordinate axis   |
| $\beta$    | Constant   |
| $\gamma$   | Rate coefficient ( $s^{-1}$ or $m^{-1}$ )  |
| $\delta$   | Ratio between the amplitudes of longshore sand transport rate in two neighboring solution areas        |
| $\Delta$   | Change in quantity   |
| $\epsilon$ | Coastal constant (diffusion coefficient) ( $m^2/sec$ )   |
| $\zeta$    | Integration limit in the complex plane having all singularities of the integrated function to the left |
| $\lambda$  | Porosity of sand   |
| $\xi$      | Integration variable   |
| $\rho$     | Density of water ( $kg/m^3$ )  |

|          |  |
|----------|--|
| $\rho_s$ | Density of sand ( $\text{kg/m}^3$ )                    |
| $\sigma$ | Wave number of periodic beach cusps ( $\text{rad/m}$ ) |
| $\tau$   | Integration variable                                   |
| $\phi$   | Phase angle  |
| $\omega$ | Angular frequency ( $\text{rad/sec}$ )                 |

Subscripts: Denoting various specific values of a variable or various solution areas

1, 2, 3...

i, j, m

H, v

Superscripts: Denoting various specific values of a variable or various solution areas

1, 2, 3...

a, b, m, v

R, L

Mathematical symbols

|            |                         |
|------------|-------------------------|
| d          | Differentiation         |
| $\partial$ | Partial differentiation |
|            | Absolute value          |





